Disturbance Triggers Non-Linear Microbe-Environment Feedbacks

Aditi Sengupta[1†], Sarah J. Fansler[2†], Rosalie K. Chu[3], Robert E. Danczak[2], Vanessa A. Garayburu-Caruso[2], Lupita Renteria[2], Hyun-Seob Song[4], Jason Toyoda[3], Jacqueline Wells[5], and James C. Stegen[2*]

[†]Denotes equal contribution

[1]California Lutheran University, Thousand Oaks, CA

[2]Pacific Northwest National Laboratory, Ecosystem Science Team, Richland, WA

[3]Environmental Molecular Sciences Laboratory, Richland, WA

[4]University of Nebraska-Lincoln, Lincoln, NE

[5]Oregon State University, Corvallis, OR

Correspondence to: James Stegen (James.Stegen@pnnl.gov)

Abstract

Conceptual frameworks linking microbial community membership, properties, and processes with the environment and emergent function have been proposed but remain untested. Here we refine and test a recent conceptual framework using hyporheic zone sediments exposed to wetting/drying transitions. Our refined framework includes relationships between cumulative properties of a microbial community (*e.g.* microbial membership, community assembly properties, and biogeochemical rates), environmental features (*e.g.* organic matter thermodynamics), and emergent ecosystem function. Our primary aim was to evaluate the hypothesized relationships that comprise the conceptual framework and contrast outcomes from the whole and putatively active bacterial and archaeal communities. Throughout the system we found threshold-like responses to the duration of desiccation. Membership of the putatively active bacterial community--but not the whole bacterial and archaeal community--responded due to enhanced deterministic selection (an emergent community property). Concurrently, the thermodynamic properties of organic matter (OM) became less favorable for oxidation (an environmental component) and respiration decreased (a microbial process). While these responses were step functions of desiccation, we found that in deterministically assembled active communities, respiration was lower and thermodynamic properties of OM were less favorable. Placing the results in context of our conceptual framework points to previously

27 unrecognized internal feedbacks that are initiated by disturbance, mediated by thermodynamics, and that

28 cause the impacts of disturbance to be dependent on the history of disturbance.

29

30 1 Introduction

31 1.1 Conceptual Foundations

32 Given the influence of microbes over ecosystem function, deeper knowledge of microbe-environment

33 relationships is needed to improve ecosystem models (Bier et al., 2015). In turn, there is strong interest

34 in quantifying and predicting microbe-environment relationships such as defining microbial life history

35 strategies as traits in ecosystem models (Malik et al., 2020), assessing microbial biomass stoichiometry

36 distributions in response to changing resource environments (Manzella et al., 2019), and evaluating the

37 extent of microbial adaptation to changing environments and their role in biogeochemical processes

38 (Wallenstein and Hall, 2012). To enhance and synthesize understanding of microbe-environment

39 interactions, it is useful to develop conceptual frameworks based on linkages among microbial

40 characteristics and ecosystem processes. Previous work has used such frameworks to improve

41 mechanistic representation and predictive capacity of microbe-environment interactions in ecosystem

42 models (Wieder et al., 2015).

43

44 A recently developed framework by Hall et al. (Hall et al., 2018) poses a series of concepts that

45 collectively define the intersection between microbial and ecosystem ecology. Their framework draws

46 attention to causal relationships between microbial characteristics (microbial membership influences

47 community properties and microbial processes), which in turn regulate ecosystem fluxes. These

48 components can be further modified by environmental variation leading to cumulative ecosystems

49 processes with the potential to incorporate relevant mechanistic links into predictive ecosystem models.

Hall et al. (2018) particularly draws attention to the need to understand how microorganisms influence their environment by separating microbial community properties based on community aggregated traits (those which can be predicted using constituent taxa) and emergent properties (properties unable to be explained by constituent taxa). -A powerful element of the framework is that it applies to diverse systems spanning natural (Gilbert et al., 2018), host-associated (Lloyd-Price et al., 2019), and built (Fu et al., 2020) environments as well as across spatiotemporal scales (König et al., 2018). While potentially very useful, the Hall et al. (2018) framework has seen little direct use in terms of explicitly defining and evaluating the linkages within specific study systems (but see Manzella et al., 2019). To make full use of and continually improve the framework, it is necessary to consider different realizations and interpretations of the proposed linkages. In the following paragraphs we detail a modified interpretation of the framework (**Fig. 1**) to enable its application to microbial communities and biogeochemistry associated with hyporheic zone sediments experiencing hydrological disturbance. In turn, we use data from a controlled laboratory experiment to evaluate key linkages within the modified framework.

Our modified framework aims to refine the link between microbial communities and ecosystem functions. As detailed below, a couple critical elements of our modification include: Defining and evaluating the relative influence of community assembly processes as an emergent community property, and ii) proposing bi-directional links between environment and microbial processes to indicate that environmental conditions drive microbial processes, which in turn influence the environment, and these cumulative environment-microbial processes ultimately drive ecosystem function.

1.2 Conceptual Framework Development

73   As in Hall et al. (2018) we consider microbial membership to be directly influenced by environmental

74   conditions (arrow 4, Fig.1) and to underlie community-level properties (arrow 1, Fig. 1). Determining

75   microbial membership is relatively straightforward, and uses culture-independent (Behrens et al., 2012;

76   Norland et al., 1995; Thompson et al., 2017; Wagner, 2009) and culture-dependent (Bartelme et al.,

77   2020) techniques. Sequence-based assays using phylogenetic markers are routine, with DNA-based

78   (total community members) and RNA-based (putatively active community members) (Barnard et al.,

79   2015; Blazewicz et al., 2013; Cardoso et al., 2017; Kearns et al., 2016; Shu et al., 2019; Wisnoski et al.,

80   2020) approaches providing the foundation to study community properties.

81

82   While community membership is relatively straightforward, the identification of community properties

83   that are relevant to a given system and function is open to broader interpretation. Here we propose using

84   the relative influences of deterministic and stochastic community assembly processes (Stegen et al.,

85   2012) as emergent properties of microbial communities that have implications for biogeochemical

86   function (Graham and Stegen, 2017) including in ecosystems experiencing environmental disturbance.

87   Deterministic mechanisms are associated with systematic differences in reproductive success imposed

88   by the biotic and/or abiotic environment, while stochastic mechanisms are associated with passive

89   spatial movements of organisms and birth/death events that are not due to systematic differences across

90   taxa in reproductive success (Dini-Andreote et al., 2015; Stegen et al., 2015). The relative contributions

91   of determinism and stochasticity can be inferred by coupling microbial community membership and

92   phylogeny to ecological null models (Stegen et al., 2012, 2013, 2015; Zhou and Ning, 2017).

93

94   We propose that the relative contributions of determinism and stochasticity are emergent properties that

95   are greater than the sum of the individual components (i.e., taxa), and that are complementary to the

96 community properties proposed by Hall et al. (Hall et al., 2018), such as biomass and gene expression.

97 Furthermore, we propose that there are feedbacks between assembly processes and microbial

98 membership whereby assembly processes influence which taxa are found in which abundances, but

99 biotic interactions also influence assembly processes. In turn, we modified the framework whereby

100 arrow 1 is bidirectional (Fig. 1).

101

102 It is important to recognize that the ecological processes of community assembly are distinct from

103 'microbial processes' associated with biogeochemical reactions. As an emergent property, the relative

104 influence of determinism and stochasticity is the result of complex biotic and abiotic interactions (Grilli

105 et al., 2017) and also shapes cumulative microbial processes that impact ecosystem biogeochemical

106 functions (Graham and Stegen, 2017) (arrow 2, Fig.1). For example, a stronger influence of determinism

107 over community assembly is hypothesized to cause higher respiration rates (a microbial processes) due

108 to a larger contribution of well-adapted taxa (Graham and Stegen, 2017), though the respiration response

109 may vary depending on the existing community composition and the deterministic forces exerted.

110

111 Analyses of microbial community assembly have been widely employed across environments including

112 soil (Bottos et al., 2018; Dini-Andreote et al., 2015; Feng et al., 2018; Jurburg et al., 2017; Sengupta et

113 al., 2019b), sediment (Graham et al., 2017a; Stegen et al., 2013, 2016, 2018b), marine (Starnawski et al.,

114 2017; Wu et al., 2018), riverine (Chen et al., 2019), gut (Martínez et al., 2015), and engineered (Ofiţeru

115 et al., 2010; Zhou et al., 2013) systems. Previous work has focused primarily on using DNA-derived

116 membership and phylogenetic data to study whole-community assembly. In contrast, recent studies have

117 also used an RNA-based approach to study the relative influence of stochasticity over the assembly of

118 the putatively active portion of microbial communities (Jia et al., 2020; Jurburg et al., 2017). This RNA-

119 based approach is complementary to the DNA-based approach and may provide additional insights into

120 shorter-term dynamic linkages between emergent community properties and microbial processes. Such

121 linkages have not, however, been previously evaluated.

122

123 The Hall et al. (2018) framework proposes that microbial processes (e.g., respiration rate) are

124 influenced by both microbial community properties and environmental factors. Here we propose a

125 revision of this structure that includes bidirectional links between the environment and microbial

126 processes (arrow 3, Fig. 1). Such bi-directional links between microbes and their environment are

127 common (Daly et al., 2016; Leventhal et al., 2019; Ratzke et al., 2018; Stegen et al., 2018a), and in

128 hyporheic zone sediments may be particularly tied to thermodynamic properties of organic matter

129 (Graham et al., 2018) and influenced by hydrological disturbances that are common in such

130 environments. For example, preferential use of OM by microbial communities has potential to alter the

131 thermodynamic properties of organic matter pools (Graham et al., 2017a). This microbe-driven shift in

132 the environment could then feedback to impact microbial metabolism due to the strong influence of OM

133 thermodynamics on biogeochemical rates (Boye et al., 2017; Garayburu-Caruso et al., 2020; Song et al.,

134 2020; Stegen et al., 2018b). Bi-directional feedback between environmental factors and microbial

135 processes is, therefore, likely important to the link between microbial communities and ecosystem

136 function. Fundamental knowledge of these feedbacks and how they are modulated by hydrologic

137 disturbances in hyporheic zone sediments is largely unknown, however.

138

139 Within ecosystems, mechanistic associations between environmental factors, microbial properties, and

140 microbial processes underlie spatial and temporal distributions of biogeochemical rates (Fig. 1 arrow 5).

141 The resulting distributions (e.g., of respiration rates) define cumulative system function and can be used

142   to understand key phenomena such as biogeochemical hot spots and hot moments (McClain et al.,

143   2003). Developing concepts and models to predict the influences of biogeochemical hot spots/moments

144   is a major outstanding challenge. To facilitate progress, Bernhardt et al. (2017) proposed grouping hot

145   spots/moments into the concept of ecosystem control points that exert a disproportionate influence on

146   ecosystem function.

147

148   While not called out explicitly in Bernhardt et al. (2017), the control point concept is based on the

149   distribution of biogeochemical rates through space and/or time. Focusing on the shape of rate

150   distributions allows the notion of control points to be extended to the concept of control point influence

151   (CPI; Fig. 1 arrow 5). The CPI is a quantitative measurement of the contribution of elevated

152   biogeochemical rates in space and/or time to the net aggregated rate within a defined system (Arora et

153   al., 2020). While proposed conceptually and studied via simulation in Arora et al. (2020), empirical

154   measurements of CPI are lacking. More generally, incorporating CPI into a modified version of the Hall

155   et al. (2018) framework (Fig. 1), provides an integrated conceptualization for how environmental

156   factors, microbial properties, and microbial processes contribute to emergent system function.

157

158   Some elements of our modified framework (Fig. 1) are generalizable across systems (e.g., CPI), while

159   others (e.g., OM thermodynamics) may have different levels of relevance across different ecosystem

160   types. Here we aim to generate fundamental knowledge of the linkages between microbial community

161   and ecosystem function, as well as reveal how hydrologic disturbance may modify these linkages. While

162   relationships between microbial community assembly and function have been evaluated, integrating the

163   concepts of microbial structure, function, assembly, and environment interactions into one coherent

164 framework has the potential to advance our understanding of the feedbacks between microbial

165 communities and the environment.

166

167 1.3 Study Objectives

168 Our primary objective was to study the modified conceptual framework in context of variably inundated

169 hyporheic zone sediments exposed to different drying/wetting dynamics. Hyporheic zones are

170 biogeochemically active subsurface domains in river corridors through which surface water flows and

171 can mix with groundwater (Bernhardt et al., 2017; Boano et al., 2014; McClain et al., 2003). These

172 zones can have disproportionate biogeochemical impacts on river corridors (Boano et al., 2014; Burrows

173 et al., 2017; Demars, 2019; Fischer et al., 2005; Kaufman et al., 2017). Within variably inundated

174 streams (Larned et al., 2010; Romaní et al., 2006), hyporheic zones experience extreme changes in

175 environmental conditions, but the consequences of this variability for microbe-ecosystem linkages is

176 poorly known.

177

178 To mimic natural disturbances, we subjected sediments to wetting-drying transitions and focused on a

179 series of analyses tied to our modified framework. We specifically evaluated relationships between: (*i*)

180 the relative influence of stochastic assembly as a community property and respiration rates as a

181 microbial process (Fig. 1 arrow 2), and (*ii*) environmental features and both microbial properties (Fig. 1

182 arrow 4) and processes (Fig. 1 arrow 3) that underlie aggregate system function (Fig. 1 arrow 5). We

183 evaluated relationships between cumulative properties of the microbial community (membership,

184 assembly, biogeochemical rates), environmental features, and emergent ecosystem function by

185 hypothesizing that: (*i*) Stronger influences of determinism result in well-adapted microbes that will

186 generate higher respiration rates, (*ii*) Longer duration in an inundated state will result in greater

187 influences of stochastic assembly--due to weaker ecological selection--and lower respiration rates

following re-inundation due to relatively consistent abiotic conditions (Birch, 1964), ~~and~~ (*iii*) Microbial

processes are facilitated by OM that is thermodynamically more favorable for oxidation, leading to an

association between respiration rates and OM thermodynamics, and (*iv*) More wet/dry transitions will

increase among-replicate heterogeneity (e.g., in microbial membership) thereby increasing CPI by

increasing within-treatment variability in respiration rates.

2 Methods

2.1 Study site and sediment collection

Hyporheic sediments were collected from the Columbia River shoreline (approximately 46.372411°N,

119.271695°W) in eastern Washington State (Fig S1) (Arntzen, 2006; Goldman et al., 2017; Graham et

al., 2016; Slater et al., 2010; Stegen et al., 2018b; Zachara et al., 2013) within the Hanford Site on

January 14, 2019 at 9 am Pacific Standard Time. Samples were aseptically collected to a depth of 10 cm

at five sub-sampling locations within a meter to form a composite sample that was sieved on site

through a 2 mm sieve into a clean glass beaker. Sieved sediment was stored on blue ice for 30 min while

being transported back to the laboratory. Once back at the laboratory sediment was stored at 4 °C until

processing into incubation vials (see below).

The sediments were subjected to increasing temporal environmental variance (as a function of periodic

wetting and drying transitions) and evaluated for associations between microbial membership, microbial

properties, microbial community assembly, OM chemistry, absolute respiration rate (represented in this

study as O_2 consumption rates), and cumulative respiration rates represented as CPI. Aerobic respiration

was chosen as the biogeochemical process since it influences global-scale energy and material fluxes

210 (Fatichi et al., 2019), and because the hyporheic zone within the field system is predominantly aerobic

211 (Graham et al., 2016, 2017b). Detailed experimental design and methods are provided in the following

212 paragraphs.

213

2.2 Experimental design

215 Sediments used in the batch reactors were sourced from one homogenized sediment pool. In turn, 10 g

216 of sediment from the homogenized pool was added to each reactor vial. The sample set was then split

217 into two groups, one inundated and the other allowed to desiccate. Desiccation was achieved within 15-

218 17 days. Sediments were periodically weighed to allow the inundated samples to be maintained at a

219 constant water content and to monitor the remaining samples for desiccation. Inundated sediments were

220 placed on ceramic porous plates saturated with DI water for weight adjustments. These conditions were

221 maintained for 23 days prior to the start of dynamic moisture manipulation, from January 29th to

222 February 21st, 2019. This initial 'preconditioning' period was used to avoid measuring the immediate

223 impacts of sampling disturbance and to allow time for desiccation. All replicate reactors were

224 maintained in the dark, shaking at 100 rpm, at 21 ºC and were covered with a gas permeable Breathe-

225 Easy (Milli-Pore Sigma, Burlington, MA) membrane that allowed for gas exchange and drying. After

226 the preconditioning period in which sediments were consistently inundated or allowed to continuously

227 desiccate, the transition regimes (**Fig. 2**) were applied to the reactors starting on February 22nd, 2019.

228 We refer to the time from Feb 22nd, 2019 onwards as the 'transitions period' for all treatments, even

229 though some did not experience transitions between being inundated and dry. Each treatment had 6-7

230 replicates (detailed below). These regimes were designed around the number of wet/dry transitions

231 experienced by sediments within a given treatment. Treatment regimes also caused variation in the

232 cumulative number of days sediments were in a drying state. We imposed six different experimental

233 treatment regimes (**Fig. 2**) as follows:

- 234   0 Transitions and 0 days of desiccation: Sediments were maintained at field moisture conditions
- 235   for the preconditioning and transitions periods. This treatment had 6 replicates.

- 236   1 Transition and 34 days of desiccation: Sediments were dry during the preconditioning and
- 237   transitions periods, and transitioned once to the field moisture level prior to respiration
- 238   estimation. This treatment had 6 replicates.

- 239   2 Transitions and 4 days of desiccation: Sediments were held at field moisture levels for the
- 240   preconditioning period and then for the first 7 days of the transitions period, then transitioned to
- 241   a dried state for 4 days, and transitioned to field moisture conditions prior to respiration
- 242   estimation. This treatment had 7 replicates.

- 243   3 Transitions and 31 days of desiccation: Sediments were dry during the preconditioning period
- 244   and the first 4 days of the transitions period, then transitioned to field moisture levels for three
- 245   days, then transitioned to 4 days in a dried state, and transitioned again to field moisture levels
- 246   prior to respiration estimation. This treatment had 7 replicates.

- 247   4 Transitions and 8 days of desiccation: Sediments were held at field moisture levels for the
- 248   preconditioning period and transitioned to a dried state for the first 4 days of the transitions
- 249   period, then transitioned to field moisture levels for 3 days, then transitioned to 4 days in a dried
- 250   state, and transitioned to field moisture levels prior to respiration estimation. This treatment had
- 251   7 replicates.

- 252   5 Transitions and 27 days of desiccation: Sediments were dry during the preconditioning period
- 253   and then transitioned to field moisture levels for the first 3 days of the transitions period,
- 254   transitioned to a dried state for 2 days, transitioned to field moisture levels for 2 days,

255   transitioned to a dried state for 2 days, and transitioned to field moisture levels for 3 days prior to

256   respiration estimation. This treatment had 7 replicates.

257

258   To avoid modifying electrical conductivity across experimental treatments, sterile deionized water was

259   added to reactors to achieve/maintain field moisture levels according to the defined wet/dry regimes

260   detailed above. For reactors with sediments that were below field moisture levels, deionized water was

261   added to achieve field moisture levels prior to respiration rate estimation. Changes in the total mass of

262   reactors and volumes of water added during the course of the experiment are provided in Table S1.

263

264   2.3 Respiration rate measurements

265   Laboratory incubations were performed in batch reactors to quantify dissolved oxygen consumption

266   rates. Borosilicate glass vials (20 ml) (I-Chem™ Clear VOA Glass Vials, Thermo-Fisher, Waltham,

267   MA) served as incubator reactors. Factory calibrated oxygen sensor spots (Part# 200001875, diameter =

268   0.5 cm, detection limit 15 ppb, 0 – 100 % oxygen; PreSens GmbH, Regensburg, Germany) were adhered

269   to the inner vials of the reactor prior to sediment addition. Detailed description of sensor adhesion and

270   non-destructive measurements of DO consumption using these sensors is provided in Garayburo-Caruso

271   et al. (Garayburu-Caruso et al., 2020). Vials were grouped into six treatment regimes (explained in the

272   previous section) representing inundation-drought transitions.

273

274   Sample processing and incubations were performed in a laboratory at 21±1 °C. The reactors were

275   monitored for 2 hours, with measurement of dissolved oxygen (DO) concentration (μmol L^{-1}) every 30

276   min. DO concentration in each bioreactor was measured with an oxygen optical meter (Fibox 3;

277 PreSens GmbH) connected to a 2 mm polymer optical fiber lined up to sense the sensor dot every thirty

278 minutes. Respiration rates (μmol L^{-1} h^{-1}) were estimated as the slope of the linear regression between

279 DO concentration and incubation time for each sample. Some non-linearity was observed in the

280 relationship between DO concentration and time such that only the first 4 data points--time zero to 2

281 hours--were used to fit a linear function. The slope of the linear function was taken as an estimate of

282 respiration rate.

283

2.4 Microbial Analysis

285 Post-incubation, the sediment slurry was transferred to centrifuge tubes (Item#28-108 Genesee

286 Scientific) and centrifuged for 5 min at 3200 rcf and 20°C. The supernatant was removed and reserved

287 for biogeochemistry analyses and sediment aliquots for DNA and RNA extraction were flash-frozen in

288 liquid N$_2$ and stored at −80 °C. The extraction, purification, and sequencing of sediment microbial

289 gDNA were performed according to published protocol (Bottos et al., 2018). The extraction of RNA was

290 performed using the Qiagen PowerSoil RNA extraction kit (Qiagen, Germantown, MD). RNA was

291 treated with DNase and quantified with a Qubit RNA kit (Thermo Fisher, Waltham, MA). An aliquot of

292 the RNA extraction was used to generate cDNA using SuperScript™ IV First-Strand Synthesis System

293 (Thermo Fisher Scientific, Waltham, MA). The 16S rRNA gene sequencing--for both gDNA and

294 cDNA--followed the established protocol by The Earth Microbiome Project (Caporaso, 2018). Sequence

295 pre-processing, operational taxonomic unit (OTU) assignment, and phylogenetic tree building were

296 performed using an in-house pipeline, HUNDO (Brown et al., 2018). Sequences were deposited at

297 NCBI's Sequence Read Archive PRJNA641165. The final sample count of gDNA and cDNA,

298 respectively, for each treatment regime, after dropping samples following quality filtering and

299   rarefaction, was 5 and 5 (0 transition), 4 and 3 (1 transition), 5 and 4 (2 transitions), 7 and 6 (3

300   transitions), 7 and 6 (4 transitions), and 7 and 5 (5 transitions). Rarefaction levels are provided below in

301   the Statistics section.

302

303   2.5 Biogeochemistry

304   Reserved supernatant was filtered through a 0.22 μm polyethersulfone membrane filter (Millipore

305   Sterivex) and an aliquot was immediately removed for non-purgeable organic carbon (NPOC) and the

306   remainder was stored at -20C until further OM high resolution analysis was conducted (see below).

307   NPOC was determined by acidifying an aliquot of sample with 15% by volume of 2N ultra-pure HCL

308   (Optima grade, Fisher#A466-500). The acidified sample was sparged with carrier gas (zero air, Oxarc#

309   X32070) for 5 minutes to remove the inorganic carbon component. The sparged sample was then

310   injected into the TOC-L furnace of the Shimadzu combustion carbon analyzer TOC-L CSH/CSN E100V

311   with ASI-L auto sampler at 680°C using 150 uL injection volumes. The best 4 out of 5 injections

312   replicates were averaged to get the final result. The NPOC ~~organic carbon~~ standard was made from

313   potassium hydrogen phthalate solid (Nacalia Tesque, lot M7M4380). The calibration range was 0 to 70

314   ppm NPOC as carbon.

315   Fourier Transform Ion Cyclotron Resonance Mass Spectrometry (FTICR-MS) of post-incubation

316   sediment slurry was conducted as per Danczak et al. (2020). Sample processing, injection, and data

317   acquisition, processing and analysis was performed as per scripts provided in Danczak et al. (2020), with

318   '*Start tolerance*' in Formularity changed to 8. Ten samples were dropped due to poor calibration,

319   resulting in 5 replicates for 0 transition, 4 replicates for 1 transition, 5 replicates for 2 transitions, 6

320   replicates for 3 transitions, and 5 replicates each for 4 and 5 transition regimes.

321

322   From the FTICR-MS data, as in previous work (Garayburu-Caruso et al., 2020; Graham et al., 2018;

323   Sengupta et al., 2019b; Stegen et al., 2018b), we followed LaRowe and Van Cappellen (LaRowe and

324   Van Cappellen, 2011) to calculate the Gibbs free energy for the half reaction of organic carbon

325   oxidation under standard conditions (ΔG^0_{Cox}). This calculation is based on elemental stoichiometries

326   associated with molecular formulae assigned to individual molecules observed in the FTICR-MS data.

327   The formulae assignments are part of the processing scripts described in (Danczak et al., 2020). As in

328   previous work (Garayburu-Caruso et al., 2020; Graham et al., 2018; Sengupta et al., 2019b; Stegen et

329   al., 2018b), we interpret larger values of ΔG^0_{Cox} to indicate OM that is thermodynamically less favorable

330   for oxidation by microbes. That is, larger values of ΔG^0_{Cox} indicate OM that provides less net energy to a

331   microbial cell per oxidation event, assuming all else is equal. Given the large numbers of assigned

332   formulae within each sample, this resulted in thousands of ΔG^0_{Cox} estimates within each sample, from

333   which we estimated mean ΔG^0_{Cox} for each sample.

334

2.6 Estimating influences of community assembly processes

336   The relative influences of community assembly processes impacting microbial community membership

337   are emergent properties that cannot be calculated/inferred directly from knowledge of membership. To

338   evaluate assembly processes as a link between membership and microbial processes (refer Fig. 1) it is

339   necessary to quantitatively estimate the relative influences of these processes. To do so we use a well-

340   established null modeling framework based on phylogenetic relationships among microbial taxa (Dini-

341 Andreote et al., 2015; Stegen et al., 2012, 2015; Zhou and Ning, 2017). We refer the reader to these

342 previous studies for details. In brief, randomizations were used to generate estimates of phylogenetic

343 associations among microbial taxa for scenarios in which microbial communities were stochastically

344 assembled. These stochastic (i.e., null) expectations were compared quantitatively to observed

345 phylogenetic associations to estimate the β-Nearest Taxon Index (βNTI) (Stegen et al., 2012). We used

346 cDNA sequences rarefied to 27227 and gDNA sequences rarefied to 15106 sequences per sample to

347 determine putatively active community and whole community βNTI values, respectively. Samples

348 falling below these sequence counts were removed as indicated above in subsection *2.4 Microbial*

349 *Analysis.* A βNTI value of 0 indicates no deviation between the stochastic expectation and the observed

350 phylogenetic associations, thereby indicating the dominance of stochastic assembly processes. As βNTI

351 deviates further from 0, there is an increasing influence of deterministic assembly processes that drive

352 community membership away from the stochastic expectation. βNTI values below -2 or above +2

353 indicate statistical significance, with negative and positive values indicating less than or more than

354 expected shifts in membership. βNTI is a pairwise metric measured between any two

355 communities/samples, such that shifts in membership are related to changes between the pair of

356 communities being evaluated. We used βNTI to study all pairwise community comparisons within each

357 experimental treatment. Each community from a given reactor is therefore associated with multiple

358 βNTI values due to being compared to communities associated with other replicate reactors. In turn, the

359 average βNTI was calculated for each reactor. As in Stegen et al. (Stegen et al., 2015), this provides a

360 community-specific value for βNTI and thus an estimate of the relative influences of stochastic and

361 deterministic processes causing deviations between a given community and all other communities within

362 the same experimental conditions (Sengupta et al., 2019b). That is, the larger the absolute value of βNTI

363 for a given community, the stronger the influence of deterministic assembly processes acting on that

364 community (Stegen et al., 2015). In turn, these community-specific estimates were related to reactor-

365 specific measurements. For example, respiration rates were regressed against βNTI to evaluate the link

366 between emergent properties (i.e., ecological assembly) and microbial processes (i.e., respiration rates).

367

2.7 Evaluating relationships between microbial characteristics and

environment

370 Respiration rate distributions, absolute βNTI values, and ΔG^0_{Cox} were summarized as box plots.

371 Pairwise Mann-Whitney test was performed to evaluate statistical differences between reactor-specific

372 measurements (*e.g.*,respiration rates and thermodynamic properties) and treatment groups (cumulative

373 dry and inundated days). Continuous bivariate relationships were evaluated with ordinary least squares

374 regression. Prior to regression analyses, respiration rates were log-transformed due to non-linearities

375 resulting from respiration being constrained to be at or above zero. Prior to log-transformation, half the

376 smallest non-zero rate was added to each rate to enable inclusion of rate estimates with a value of zero.

377

2.8 Control point influence calculation

379 To characterize respiration rate distributions we used the control point influence (CPI) metric. CPI was

380 recently developed (Arora et al., 2020) and is defined as the fraction of cumulative function (R_{tot}; e.g.,

381 total respiration rate) within a defined system that is contributed by individual rates that are above the

382 system's median rate (R_{med}). To define cumulative function one must first define the system being

383 evaluated. In our study, all replicate batch reactors within a given experimental treatment were

384 conceptualized as a representative set of samples from a larger system experiencing the experimental

385   conditions. R_{tot} for each treatment was therefore estimated as the sum of respiration rates across a

386   treatment's replicate reactors. CPI was estimated as the sum of respiration rates that fell above the

387   median rate for a given treatment (R_{above}) divided by R_{tot} for that treatment. That is, $R_{above} = \sum_{i}^{N} R_{i}$,

388   where R_i are respiration rates from individual reactors that fell above R_{med}, and $CPI = R_{above} / R_{tot}$.

389

390   An important feature of CPI is that it makes no assumptions of distribution normality, and can be

391   estimated for rate distributions of any form (e.g., unimodal, multimodal, Gaussian, skewed, etc.). In

392   most cases, CPI is constrained to have a minimum value of 0.5 (for a perfectly normal distribution with

393   no outliers) and asymptotically approach 1 as a maximum value (e.g., for heavily skewed distributions

394   with a small number of very high rates). CPI therefore quantitatively estimates the biogeochemical

395   contribution of places in space or points in time that have elevated biogeochemical rates.

396

397   Understanding how CPI varies through space, time, and with environmental conditions (e.g., disturbance

398   frequency) provides an opportunity to deepen our understanding of factors controlling hotspot/moment

399   behavior. Lower values of CPI (i.e., closer to 0.5) can arise through any mechanism that constrains

400   biogeochemical rates to be consistent through space or time. For example, if respiration rates were

401   measured in multiple locations across a well-mixed water body, we may expect a Gaussian rate

402   distribution with little variation. The cumulative respiration of the water body should not be influenced

403   significantly by hotspots, which would be reflected in low CPI. Conversely, higher values of CPI (i.e.,

404   closer to 1) can arise through any mechanism that increases the probability of positive outliers within a

405   given rate distribution. Spatial variation in the temporal dynamics of disturbances (e.g., more frequent

406   disturbances in some locations) is an example that is closely aligned with our experimental treatments.

407   In this case the probability of rate outliers (i.e., hotspots) may vary as a function of disturbance

17

408   frequency. For example, in spatial domains that experience more wetting/drying dynamics we might

409   expect a higher probability of rate outliers. This is because each time sediments go dry the exact spatial

410   distribution of water films that remain will vary across locations within the broader wetted/dried spatial

411   domain. In turn, we would expect higher values of CPI in spatial domains that are more frequently

412   wetted and dried. Regardless of whether this specific hypothesis is rejected or not, we contend that using

413   CPI enables development of *a priori* quantitative hypotheses spanning space, time, environmental

414   conditions (e.g., disturbance frequency), and scales. This provides new opportunities to more

415   systematically elucidate factors governing the influence of hotspots/moments.

416

3 Results

418   To link microbial membership to emergent microbial community properties (Fig. 1 arrow 1) we used

419   null modeling to estimate the contributions of stochastic and deterministic community assembly. Results

420   from the null models indicate a relatively balanced mixture of stochasticity and determinism for both the

421   whole community (gDNA-based) and putatively active community (rRNA-based) (Fig. S2). More

422   specifically, stochasticity and determinism each governed 50% of turnover in microbial membership for

423   the whole community and 33% and 67%, respectively, for the putatively active community. The relative

424   contributions of the two deterministic components (homogeneous and variable selection) were strongly

425   imbalanced. Homogeneous selection was responsible for 94% and 91% of the deterministic component

426   for the whole and putatively active communities, respectively. The contributions of homogeneous and

427   variable selection to the deterministic component must sum to 1, such that the variable selection was

428   responsible for 6% and 9% of the deterministic component for the whole and putatively active

429   communities, respectively.

430

431 As shown in Figure 1 (arrow 2), we hypothesized a link between microbial community properties and

432 microbial processes realized as a relationship between the strength of determinism and respiration rates.

433 Such a relationship was not observed for the whole community (Fig. 3a), but we did observe a non-

434 linear decreasing relationship between respiration rates and the absolute value of βNTI for the putatively

435 active community (Fig. 3b). The direction of this relationship (negative) was opposite of that expected,

436 and the relationship was clearly structured by among-treatment shifts in both respiration rate and βNTI

437 (Fig. 3b).

438

439 In our conceptual framework there are multiple ways in which connections among the environment,

440 microbial properties, and microbial processes may be realized, in part due to the environment having

441 multiple components relevant to our study (Fig. 1 arrows 3,4). More specifically, the environment was

442 characterized here in terms of both disturbance (number of dry days; imposed by the experimental

443 manipulation) and OM thermodynamics (ΔG^0_{Cox}; this is an emergent aspect of the environment).

444

445 Disturbance influenced both microbial properties and processes. These influences appeared to be non-

446 linear with experimental treatments associated with the two largest number of dry days (31 and 34)

447 causing decreases in respiration rates (Fig. 4a) and stronger influences of deterministic homogeneous

448 selection for the putatively active community (Fig. 4b). Disturbance had no clear influence on

449 community assembly for the whole community (Figs. S3, S4a). Given the apparent binary nature of

450 these results, we evaluated statistical significance by combining respiration rate data from treatments

451 with 0-27 cumulative dry days and separately combining data from treatments with 31 or 34 cumulative

452 dry days (Fig. S5). Respiration rates were significantly depressed in the treatments associated with 31 or

453   34 cumulative dry days ($W = 5$, $p < 0.001$). The βNTI data are non-independent due to being based on

454   all pairwise comparisons within a treatment. Standard statistical tools are therefore not applicable for

455   assigning statistical significance when comparing βNTI distributions. However, as shown in Figures 4b

456   and S4b, there is an obvious shift to lower βNTI values for the putatively active community in the

457   treatments with 31 or 34 cumulative dry days.

458

459   The other aspect of the environment examined here (i.e., OM thermodynamics) also had significant

460   relationships with both microbial processes (Fig. 1, arrow 3) and properties (Fig. 1, arrow 4). More

461   specifically, respiration rates decreased significantly as a negative exponential function of increasing

462    $\Delta G^0{}_{Cox}$ ($R^2 = 0.34$; $p = 0.001$; Fig. 5a). This indicates a decrease in respiration rate as OM

463   thermodynamic properties shifted towards lower favorability for oxidation (i.e., larger values of $\Delta G^0{}_{Cox}$).

464   Similarly, we found that the strength of deterministic assembly associated with the putatively active

465   community increased linearly with $\Delta G^0{}_{Cox}$ ($R^2 = 0.40$; $p = 0.001$; Fig. 5b). The relationships were clearly

466   structured by among-treatment shifts in respiration rate, βNTI, and favorability of organic matter

467   ($\Delta G^0{}_{Cox}$). The strength of deterministic assembly associated with the whole community was unrelated to

468    $\Delta G^0{}_{Cox}$ ($p = 0.64$) (Fig. S6).

469

470   The conceptual model described in Figure 1 focuses primarily on connections among environmental

471   and/or microbial attributes, but there are potentially important relationships within attribute categories.

472   In particular, within the environmental category there is the potential for an influence of disturbance on

473   OM thermodynamics. Such an effect was found for OM thermodynamics as measured by $\Delta G^0{}_{Cox}$ (Fig.

474   5c). Using the same approach as for analyses described above, we combined data for treatments with 0-

475   27 cumulative dry days and compared that distribution to data combined across treatments with 31 or 34

476   cumulative dry days. A Mann-Whitney test comparing these distributions confirmed a significant

477   change in the ΔG^0_{Cox} distribution (W = 189, p = < 0.001)(Fig. S7).

478

479   The last component of the conceptual model considered here is the connection between microbial

480   processes occurring in a given location and cumulative system function that aggregates across locations

481   (Fig. 1, arrow 5). It is at the system level that the influence of biogeochemical hot spots (or hot

482   moments) can be evaluated. We conceptualized an aggregate system as the collection of replicate batch

483   reactors within a given experimental treatment. Based on this definition, we estimated control point

484   influence (CPI) as a measurement for the influence of biogeochemical hot spots. We observed a large

485   amount of variation in CPI across experimental treatments, but there was no clear, direct influence of the

486   treatments on CPI (Fig. 4). The largest value of CPI observed (> 0.9) was associated with the treatment

487   that imposed 31 cumulative dry days. This treatment also had the lowest median respiration rates across

488   all treatments (Fig. 4). We did not find any significant relationship (p > 0.70) between within-treatment

489   community compositions (whole and putatively-active) and CPI, suggesting that within-treatment beta-

490   dispersion of the community is not a better predictor of CPI.

491 4 Discussion

492   Mechanistic evaluation of microbe-environment interactions is fundamental to understanding microbe-

493   mediated ecosystem function. Inspired by a microbe-environment-ecosystem framework proposed by

494   Hall et al. (Hall et al., 2018) we proposed and evaluated a modified framework linking microbial

495   characteristics (membership, emergent properties, processes), the environment (disturbance, OM

496   thermodynamics), and cumulative ecosystem function (CPI) of hyporheic zone sediments. Our results

497   provide clear support for the overall conceptual framework and further point to an iterative loop among

498 OM thermodynamics, respiration rates, and microbial community assembly that can be initiated by

499 externally-imposed disturbance. Furthermore, our results indicate that the iterative thermodynamics-

500 assembly-respiration loop may be initiated through threshold-like impacts of disturbance that were

501 observed only after 31 or more cumulative days of desiccation.

502

503 We first evaluated emergent community properties as a function of microbial membership by studying

504 the relative influences of stochasticity and determinism over community assembly. Taking this

505 approach, we found fully balanced stochastic-deterministic influences over the whole community, in

506 which each contributed to 50% of the variation in community composition. The relative influences of

507 stochasticity and determinism have been quantified for many microbial systems and the estimates are

508 highly variable (Tripathi et al., 2018; Wang et al., 2013). In addition, within the deterministic

509 component of assembly, homogeneous selection had a far greater influence than variable selection.

510 Previous work has also observed a broad range of contributions from homogeneous and variable

511 selection (Fillinger et al., 2019; Graham et al., 2016; Li et al., 2019; Sengupta et al., 2019a; Whitman et

512 al., 2018). As such, the assembly-associated outcomes observed here for the whole community are not

513 unexpected relative to previous work. Very few studies, however, have examined the relative influences

514 of different assembly components over putatively active microbial communities. This focus is critical in

515 our framework since many microorganisms are inactive while the active community remains sensitive to

516 abiotic stresses and contributes to ecosystem function.

517

518 For the putatively active communities we found that across all treatments both stochasticity and

519 determinism were important, though deterministic assembly had greater influence. This deviates

520 quantitatively from the whole community in which the influences of stochasticity and determinism were

521   more balanced. The difference in assembly influences in whole- and putatively-active communities is

522   likely driven by the duration of the imposed experimental treatments (two weeks). This time period may

523   not be sufficient for birth and death events to restructure the community composition. Instead,

524   physiological responses as a function of decreases and increases in microbial activity (changes in cDNA

525   signatures) is more likely. A stronger disturbance (*e.g.,* imposing the treatments for a longer period of

526   time) may provide further insights into the impacts of disturbance on the whole community (*e.g.,* evident

527   as changes in gDNA signatures). Consistent with the whole community results, however, was the

528   dominance of homogeneous selection within the deterministic component of assembly. The strong

529   influence of homogeneous selection is likely due to selection-based constraints imposed by aspects of

530   the experimental system that did not vary across treatments. For example, mineralogy is known to

531   strongly influence microbial communities (Boyd et al., 2007; Carson et al., 2009; Doetterl et al., 2018;

532   Fauvel et al., 2019; Mauck and Roberts, 2007; Stegen et al., 2016) and was homogenized across the

533   experimental batch reactors, thereby potentially imposing homogeneous selection on both the whole and

534   putatively active communities.

535

536   Our study uniquely evaluates null-model outcomes of putatively-active community assemblies in

537   hyporheic zone sediments, where homogeneous selection was further enhanced by our experimentally

538   imposed hydrologic disturbances. Increased homogeneous selection in response to disturbance is

539   consistent with previous work in aquatic (Chase, 2007) and soil systems. For example, in a soil system,

540   disturbance led to an immediate increase in homogeneous selection for the putatively active community

541   (Jurburg et al., 2017). The strong influence of homogeneous selection on the putatively active

542   community is not always observed, however, suggesting it may be tied to acute disturbance. That is, Jia

543   et al. (2020) recently found that within a natural soil chronosequence, variable selection was stronger for

544   putatively-active communities while homogeneous selection influenced the whole community assembly.

545   Our results combined with these previous studies indicate that community assembly of putatively-active

546   members may be more closely linked to short-term environmental change than assembly of the whole

547   community.

548

549   In addition to being more sensitive to disturbance, we find that assembly of the putatively active

550   community was more strongly tied to microbial processes (i.e., respiration rate), than was the whole

551   community. A strong link between biogeochemical rates and the putatively active community is

552   consistent with previous studies (Freedman et al., 2015; Levy-Booth et al., 2019). More specifically, we

553   observed a negative relationship between respiration rate and absolute values of βNTI for the putatively

554   active community, but no relationship for the whole community. The direction of this relationship is

555   opposite to our hypothesis. While stronger selection should remove mal-adapted individuals, leading to

556   higher biogeochemical rates (Graham and Stegen, 2017), increased selection in our experiment was

557   imposed by disturbance that appeared to directly suppress respiration rates due to desiccation (Baldwin

558   and Mitchell, 2000; Manzoni et al., 2012). The simultaneous suppression of respiration and imposition

559   of stronger selection in treatments with 31 or 34 days of dry conditions (Fig. 3b) led to the negative

560   relationship between respiration and the strength of selection. The lack of such relationships when

561   considering the whole community indicates that a greater focus on assembly dynamics of putatively

562   active communities could reveal new insights into the multi-component linkages among microbes, the

563   environment, and function.

564

565   Disturbance also impacted OM thermodynamics and respiration rates, potentially initiating an iterative

566   loop among microbial assembly, microbial processes, and the abiotic environment. In this iterative loop

567 the direction of causation between OM thermodynamics and microbial processes (Fig. 1, arrow 3) is not

568 clear due to feedbacks, though we interpret a direction of causation from OM thermodynamics to

569 microbial properties in terms of community assembly (Fig. 1 arrow 4). As such, there may be a loop

570 between OM thermodynamics and microbial processes (i.e., respiration) embedded in a larger loop that

571 also includes microbial properties (i.e., community assembly). Such feedbacks are inherent in complex

572 systems and often lead to non-linear dynamics as observed here in terms of the threshold-like impact of

573 desiccation on multiple system components (Pérez Castro et al., 2019; Prosser and Martiny, 2020).

574

575 As key elements of the inferred system of feedbacks, the links among OM thermodynamic properties,

576 respiration, and desiccation found here are consistent with recent work tied to the same field system.

577 That is, Garayburu-Caruso et al. (Garayburu-Caruso et al., 2020) also showed decreasing aerobic

578 respiration with decreasing favorability for oxidation (i.e., larger values of ΔG^0_{Cox}) using sediments

579 sourced ~2 years previously from the same field system. In addition, the impacts of desiccation found

580 here are similar to Goldman et al. (Goldman et al., 2017) after re-inundation. This impact of desiccation

581 on respiration contrasts with the Birch effect (Birch and Friend, 1956) in soils whereby desiccation

582 followed by re-wetting leads to enhanced respiration. The consistency across hyporheic zone studies and

583 deviation from classical soil phenomena points to potential consistency in governing processes within

584 the hyporheic zone that deviate from processes operating in soil systems. Further evaluation is needed

585 across additional hyporheic zone systems to rigorously evaluate this inference, however.

586

587 In addition to linkages between the environment and microbial aspects of the system, our study revealed

588 connections within the environmental components of the conceptual framework. That is, greater

589 cumulative desiccation caused an increase in ΔG^0_{Cox}, indicating a significant change in OM

590 thermodynamics (Fig. 5c). While our data cannot pinpoint governing mechanism(s), we hypothesize that

591 the ΔG^0_{Cox} response may have been tied to increased ion concentration following desiccation. For

592 example, OM chemistry may have been altered due to changes in abiotic sorption, limitations of

593 microbially accessible C due to water potential constraints, and/or osmolyte production and formation of

594 extracellular polymeric substances (Fierer et al., 2003; Gionchetta et al., 2020; Homyak et al., 2018).

595

596 Irrespective of mechanisms, the shift in OM thermodynamics in response to desiccation was associated

597 with a decline in respiration. We infer a causal connection between OM thermodynamics and

598 respiration, potentially triggered by desiccation-driven shifts in OM chemistry and/or microbial

599 physiology. This causal connection is supported by recent work (Garayburu-Caruso et al., 2020) and the

600 observation of a continuous function between ΔG^0_{Cox} and respiration rate that transcended experimental

601 treatments. Desiccation therefore likely influences and may even initiate an iterative loop among OM

602 thermodynamics, microbial assembly, and biogeochemistry that underlies cumulative system function.

603

604 Cumulative system function can often be driven by ecosystem control points (Bernhardt et al., 2017),

605 but we observed relatively little indication of such behavior. That is, estimates of control point influence

606 (CPI) were relatively low across most treatments. CPI is theoretically constrained to range from 0.5-1,

607 with lower values indicating smaller influences of control points. In our study, all but one treatment had

608 CPI between ~0.5 and 0.7. The associated distributions of respiration rates did not contain obvious

609 outliers such that we interpret CPI values in the 0.5-0.7 range to be relatively low and not strongly

610 influenced by control points or biogeochemical hot spots/moments (McClain et al., 2003). The treatment

611 with 31 cumulative days of desiccation diverged from the rest in having a CPI value of ~0.9. This large

612 CPI was due to a single outlier (Fig. 5a) such that most of the cumulative respiration across reactors was

613   contributed by that single reactor. We interpret that single reactor as a biogeochemical hot spot or

614   control point within that experimental treatment. It is unclear, however, what led to such behavior as

615   disturbance did not have any systematic influence on CPI.

616

617   A strength of CPI as a metric is that it allows for direct quantitative comparisons across studies, systems,

618   and scales. Ours is the first study to estimate CPI, however, such that we cannot yet make comparisons

619   to previous work. Through future comparisons it will be possible to evaluate the strengths, weaknesses,

620   and behavior of CPI. We expect that some patterns may emerge such as CPI having a greater likelihood

621   to reach very high values (near 1) in systems with relatively low rates on average. In these conditions,

622   even a modest quantitative increase in biogeochemical rates can lead to a large proportional change such

623   that most cumulative function is from a single point in space and/or time, resulting in large CPI. We also

624   expect that some biogeochemical processes will show greater variation in CPI than others, potentially

625   due to variation in degree of functional redundancy (Louca et al., 2018). For example, processes such as

626   respiration can be performed by numerous microbial taxa (i.e., there is high functional redundancy),

627   while others are more constrained to a relatively small number of taxa (e.g., ammonia oxidation). We

628   hypothesize that CPI may be lower on average and less variable across systems and scales for

629   biogeochemical processes with greater functional redundancy. Additional work will be needed to test

630   this hypothesis.

631

632   5 Conclusions

633   In this study we coupled intrinsic characteristics of natural hyporheic zone sediments with imposed

634   constraints in the form of desiccation to evaluate an *a priori* conceptual framework modified from Hall

635 et al. (Hall et al., 2018). Our results demonstrated strong and often non-linear connections among

636 desiccation, OM thermodynamics, assembly of the putatively active microbial community, and

637 respiration rates. Collating our results points to further modification of the framework into an *a*

638 *posteriori* conceptual model containing nested feedback loops (**Fig. 6**). This conceptual model is

639 consistent with the recently proposed unification of microbial ecology around the concepts of external

640 forcing, internal dynamics, and historical contingencies (Stegen et al., 2018a). That is, we hypothesize

641 that external forcing imposed by desiccation initiates multiple internal loops that drive biological and

642 chemical dynamics that, in turn, underlie respiration responses to re-wetting that are contingent on

643 desiccation history. The development of conceptual models such as this is key to incorporating

644 additional mechanistic detail into predictive simulation models (e.g., reactive transport codes). We

645 encourage further evaluation and improvement of both our *a priori* and *a posteriori* concepts across

646 environmentally divergent conditions to generate knowledge that is transferable across systems.

647 **Code availability**

648 The R scripts used in this study are hosted on ESS-DIVE and will be provided to readers when

649 requested. Null modeling scripts were based on those available at

650 https://github.com/stegen/Stegen_etal_ISME_2013.

651 **Data availability**

652 Data are available on the ESS-DIVE archive at the following link (a data package will be

653 published prior to the manuscript being published, and the associated link will be provided).

654 Sequence data is available on NCBI's Sequence Read Archive PRJNA641165.

655 **Supplement**

656   The supplement related to this article is available online at: XXX

657   **Author contributions**

658   JCS and SF conceptualized and designed the study; JT, JW, LR, RC, SF, and VAG-C performed

659   the experiment; AS, JCS, RED, and SF analyzed data; AS, JCS, and SF drafted the manuscript

660   and all authors contributed to further writing.

661   **Competing interests**

662   The authors declare that they have no conflict of interest.

672

673   **References**

674   Arntzen, E.: Effects of fluctuating river flow on groundwater/surface water mixing in the hyporheic zone
675   of a regulated, large cobble bed river - Arntzen - 2006 - River Research and Applications - Wiley Online
676   Library, https://onlinelibrary.wiley.com/doi/abs/10.1002/rra.947, last access: 8 July 2020, 2006.
677
678   Arora, B., Briggs, M. A., Zarnetske, J., Stegen, J. C., Gomez-Velez, J., Dwivedi, D. and Steefel, C. I.:
679   Hot Spots and Hot Moments in the Critical Zone: Identification of and Incorporation into Reactive

Transport Models, in Biogeochemistry of the Critical Zone, edited by A. Wymore, W. Yang, W. Silver, B. McDowell, and J. Chorover, Springer-Nature, , 2020.

Baldwin, D. S. and Mitchell, A. M.: The effects of drying and re-flooding on the sediment and soil nutrient dynamics of lowland river–floodplain systems: a synthesis, Regul. Rivers Res. Manag., 16(5), 457–467, https://doi.org/10.1002/1099-1646(200009/10)16:5<457::AID-RRR597>3.0.CO;2-B, 2000.

Barnard, R. L., Osborne, C. A. and Firestone, M. K.: Changing precipitation pattern alters soil microbial community response to wet-up under a Mediterranean-type climate, ISME J., 9(4), 946–957, https://doi.org/10.1038/ismej.2014.192, 2015.

Bartelme, R. P., Custer, J. M., Dupont, C. L., Espinoza, J. L., Torralba, M., Khalili, B. and Carini, P.: Influence of Substrate Concentration on the Culturability of Heterotrophic Soil Microbes Isolated by High-Throughput Dilution-to-Extinction Cultivation, mSphere, 5(1), https://doi.org/10.1128/mSphere.00024-20, 2020.

Behrens, S., Kappler, A. and Obst, M.: Linking environmental processes to the in situ functioning of microorganisms by high-resolution secondary ion mass spectrometry (NanoSIMS) and scanning transmission X-ray microscopy (STXM), Environ. Microbiol., 14(11), 2851–2869, https://doi.org/10.1111/j.1462-2920.2012.02724.x, 2012.

Bernhardt, E. S., Blaszczak, J. R., Ficken, C. D., Fork, M. L., Kaiser, K. E. and Seybold, E. C.: Control Points in Ecosystems: Moving Beyond the Hot Spot Hot Moment Concept, Ecosystems, 20(4), 665–682, https://doi.org/10.1007/s10021-016-0103-y, 2017.

Bier, R. L., Bernhardt, E. S., Boot, C. M., Graham, E. B., Hall, E. K., Lennon, J. T., Nemergut, D. R., Osborne, B. B., Ruiz-González, C., Schimel, J. P., Waldrop, M. P. and Wallenstein, M. D.: Linking microbial community structure and microbial processes: an empirical and conceptual overview, FEMS Microbiol. Ecol., 91(10), https://doi.org/10.1093/femsec/fiv113, 2015.

Birch, H. F.: Mineralisation of plant nitrogen following alternate wet and dry conditions, Plant Soil, 20(1), 43–49, https://doi.org/10.1007/BF01378096, 1964.

Birch, H. F. and Friend, M. T.: Humus Decomposition in East African Soils, Nature, 178(4531), 500–501, https://doi.org/10.1038/178500a0, 1956.

Blazewicz, S. J., Barnard, R. L., Daly, R. A. and Firestone, M. K.: Evaluating rRNA as an indicator of microbial activity in environmental communities: limitations and uses, ISME J., 7(11), 2061–2068, https://doi.org/10.1038/ismej.2013.102, 2013.

Boano, F., Harvey, J. W., Marion, A., Packman, A. I., Revelli, R., Ridolfi, L. and Wörman, A.: Hyporheic flow and transport processes: Mechanisms, models, and biogeochemical implications, Rev. Geophys., 52(4), 603–679, https://doi.org/10.1002/2012RG000417, 2014.

Bottos, E. M., Kennedy, D. W., Romero, E. B., Fansler, S. J., Brown, J. M., Bramer, L. M., Chu, R. K., Tfaily, M. M., Jansson, J. K. and Stegen, J. C.: Dispersal limitation and thermodynamic constraints

726 govern spatial structure of permafrost microbial communities, FEMS Microbiol. Ecol., 94(8),
727 https://doi.org/10.1093/femsec/fiy110, 2018.
728

729 Boyd, E. S., Cummings, D. E. and Geesey, G. G.: Mineralogy Influences Structure and Diversity of
730 Bacterial Communities Associated with Geological Substrata in a Pristine Aquifer, Microb. Ecol., 54(1),
731 170–182, https://doi.org/10.1007/s00248-006-9187-9, 2007.
732

733 Boye, K., Noël, V., Tfaily, M. M., Bone, S. E., Williams, K. H., Bargar, J. R. and Fendorf, S.:
734 Thermodynamically controlled preservation of organic carbon in floodplains, Nat. Geosci., 10(6), 415–
735 419, https://doi.org/10.1038/ngeo2940, 2017.
736

737 Brown, J., Zavoshy, N., Brislawn, C. J. and McCue, L. A.: Hundo: a Snakemake workflow for microbial
738 community sequence data, PeerJ Inc., 2018.
739

740 Burrows, R. M., Rutlidge, H., Bond, N. R., Eberhard, S. M., Auhl, A., Andersen, M. S., Valdez, D. G.
741 and Kennard, M. J.: High rates of organic carbon processing in the hyporheic zone of intermittent
742 streams, Sci. Rep., 7(1), 1–11, https://doi.org/10.1038/s41598-017-12957-5, 2017.
743

744 Caporaso, J. G.: EMP 16S Illumina Amplicon Protocol, ,
745 https://doi.org/10.17504/protocols.io.nuudeww, 2018.
746

747 Cardoso, D. C., Sandionigi, A., Cretoiu, M. S., Casiraghi, M., Stal, L. and Bolhuis, H.: Comparison of
748 the active and resident community of a coastal microbial mat, Sci. Rep., 7(1), 1–10,
749 https://doi.org/10.1038/s41598-017-03095-z, 2017.
750

751 Carson, J. K., Campbell, L., Rooney, D., Clipson, N. and Gleeson, D. B.: Minerals in soil select distinct
752 bacterial communities in their microhabitats, FEMS Microbiol. Ecol., 67(3), 381–388,
753 https://doi.org/10.1111/j.1574-6941.2008.00645.x, 2009.
754

755 Chase, J. M.: Drought mediates the importance of stochastic community assembly, PNAS, 104,
756 17430–17434, https://doi.org/10.1073/pnas.0704350104, 2007.
757

758 Chen, W., Ren, K., Isabwe, A., Chen, H., Liu, M. and Yang, J.: Stochastic processes shape
759 microeukaryotic community assembly in a subtropical river across wet and dry seasons, Microbiome,
760 7(1), 138, https://doi.org/10.1186/s40168-019-0749-8, 2019.
761

762 Daly, R. A., Borton, M. A., Wilkins, M. J., Hoyt, D. W., Kountz, D. J., Wolfe, R. A., Welch, S. A.,
763 Marcus, D. N., Trexler, R. V., MacRae, J. D., Krzycki, J. A., Cole, D. R., Mouser, P. J. and Wrighton,
764 K. C.: Microbial metabolisms in a 2.5-km-deep ecosystem created by hydraulic fracturing in shales, Nat.
765 Microbiol., 1(10), 1–9, https://doi.org/10.1038/nmicrobiol.2016.146, 2016.
766

767 Danczak, R. E., Goldman, A. E., Chu, R. K., Toyoda, J. G., Garayburu-Caruso, V. A., Tolić, N.,
768 Graham, E. B., Morad, J. W., Renteria, L., Wells, J. R., Herzog, S. P., Ward, A. S. and Stegen, J. C.:
769 Ecological theory applied to environmental metabolomes reveals compositional divergence despite
770 conserved molecular properties, bioRxiv, 2020.02.12.946459,
771 https://doi.org/10.1101/2020.02.12.946459, 2020.

772

773 Demars, B. O. L.: Hydrological pulses and burning of dissolved organic carbon by stream respiration,
774 Limnol. Oceanogr., 64(1), 406–421, https://doi.org/10.1002/lno.11048, 2019.
775
776 Dini-Andreote, F., Stegen, J. C., Elsas, J. D. van and Salles, J. F.: Disentangling mechanisms that
777 mediate the balance between stochastic and deterministic processes in microbial succession, Proc. Natl.
778 Acad. Sci., 112(11), E1326–E1332, https://doi.org/10.1073/pnas.1414261112, 2015.
779
780 Doetterl, S., Berhe, A. A., Arnold, C., Bodé, S., Fiener, P., Finke, P., Fuchslueger, L., Griepentrog, M.,
781 Harden, J. W., Nadeu, E., Schnecker, J., Six, J., Trumbore, S., Van Oost, K., Vogel, C. and Boeckx, P.:
782 Links among warming, carbon and microbial dynamics mediated by soil mineral weathering, Nat.
783 Geosci., 11(8), 589–593, https://doi.org/10.1038/s41561-018-0168-7, 2018.
784
785 Fatichi, S., Manzoni, S., Or, D. and Paschalis, A.: A Mechanistic Model of Microbially Mediated Soil
786 Biogeochemical Processes: A Reality Check, Glob. Biogeochem. Cycles, 33(6), 620–648,
787 https://doi.org/10.1029/2018GB006077, 2019.
788
789 Fauvel, B., Cauchie, H.-M., Gantzer, C. and Ogorzaly, L.: Influence of physico-chemical characteristics
790 of sediment on the in situ spatial distribution of F-specific RNA phages in the riverbed, FEMS
791 Microbiol. Ecol., 95(2), https://doi.org/10.1093/femsec/fiy240, 2019.
792
793 Feng, Y., Chen, R., Stegen, J. C., Guo, Z., Zhang, J., Li, Z. and Lin, X.: Two key features influencing
794 community assembly processes at regional scale: Initial state and degree of change in environmental
795 conditions, Mol. Ecol., 27(24), 5238–5251, https://doi.org/10.1111/mec.14914, 2018.
796
797 Fierer, N., Allen, A. S., Schimel, J. P. and Holden, P. A.: Controls on microbial CO2 production: a
798 comparison of surface and subsurface soil horizons, Glob. Change Biol., 9(9), 1322–1332,
799 https://doi.org/10.1046/j.1365-2486.2003.00663.x, 2003.
800
801 Fillinger, L., Zhou, Y., Kellermann, C. and Griebler, C.: Non-random processes determine the
802 colonization of groundwater sediments by microbial communities in a pristine porous aquifer, Environ.
803 Microbiol., 21(1), 327–342, https://doi.org/10.1111/1462-2920.14463, 2019.
804
805 Fischer, H., Kloep, F., Wilzcek, S. and Pusch, M. T.: A River's Liver – Microbial Processes within the
806 Hyporheic Zone of a Large Lowland River, Biogeochemistry, 76(2), 349–371,
807 https://doi.org/10.1007/s10533-005-6896-y, 2005.
808
809 Freedman, Z. B., Romanowicz, K. J., Upchurch, R. A. and Zak, D. R.: Differential responses of total
810 and active soil microbial communities to long-term experimental N deposition, Soil Biol. Biochem., 90,
811 275–282, https://doi.org/10.1016/j.soilbio.2015.08.014, 2015.
812
813 Fu, X., Li, Y., Meng, Y., Yuan, Q., Zhang, Z., Norbäck, D., Deng, Y., Zhang, X. and Sun, Y.: Derived
814 ecological niches of indoor microbes are crucial for asthma symptoms in university dormitories,
815 bioRxiv, 2020.01.05.893529, https://doi.org/10.1101/2020.01.05.893529, 2020.
816
817 Garayburu-Caruso, V. A., Stegen, J. C., Song, H.-S., Renteria, L., Wells, J., Garcia, W., Resch, C. T.,

818   Goldman, A. E., Chu, R. K., Toyoda, J. and Graham, E. B.: Carbon Limitation Leads to Thermodynamic
819   Regulation of Aerobic Metabolism, Environ. Sci. Technol. Lett.,
820   https://doi.org/10.1021/acs.estlett.0c00258, 2020.

821

822   Gilbert, J. A., Jansson, J. K. and Knight, R.: Earth Microbiome Project and Global Systems Biology,
823   mSystems, 3(3), https://doi.org/10.1128/mSystems.00217-17, 2018.

824

825   Gionchetta, G., Oliva, F., Romani, A. M. and Baneras, L.: Hydrological variations shape diversity and
826   functional responses of streambed microbes, Sci. Total Environ., 714, 136838,
827   https://doi.org/10.1016/j.scitotenv.2020.136838, 2020.

828

829   Goldman, A. E., Graham, E. B., Crump, A. R., Kennedy, D. W., Romero, E. B., Anderson, C. G., Dana,
830   K. L., Resch, C. T., Fredrickson, J. K. and Stegen, J. C.: Biogeochemical cycling at the aquatic–
831   terrestrial interface is linked to parafluvial hyporheic zone inundation history, Biogeosciences, 14(18),
832   4229–4241, https://doi.org/10.5194/bg-14-4229-2017, 2017.

833

834   Graham, E. B. and Stegen, J. C.: Dispersal-Based Microbial Community Assembly Decreases
835   Biogeochemical Function, Processes, 5(4), 65, https://doi.org/10.3390/pr5040065, 2017.

836

837   Graham, E. B., Crump, A. R., Resch, C. T., Fansler, S., Arntzen, E., Kennedy, D. W., Fredrickson, J. K.
838   and Stegen, J. C.: Coupling Spatiotemporal Community Assembly Processes to Changes in Microbial
839   Metabolism, Front. Microbiol., 7, https://doi.org/10.3389/fmicb.2016.01949, 2016.

840

841   Graham, E. B., Tfaily, M. M., Crump, A. R., Goldman, A. E., Bramer, L. M., Arntzen, E., Romero, E.,
842   Resch, C. T., Kennedy, D. W. and Stegen, J. C.: Carbon Inputs From Riparian Vegetation Limit
843   Oxidation of Physically Bound Organic Carbon Via Biochemical and Thermodynamic Processes, J.
844   Geophys. Res. Biogeosciences, 122(12), 3188–3205, https://doi.org/10.1002/2017JG003967, 2017a.

845

846   Graham, E. B., Crump, A. R., Resch, C. T., Fansler, S., Arntzen, E., Kennedy, D. W., Fredrickson, J. K.
847   and Stegen, J. C.: Deterministic influences exceed dispersal effects on hydrologically-connected
848   microbiomes, Environ. Microbiol., 19(4), 1552–1567, https://doi.org/10.1111/1462-2920.13720, 2017b.

849

850   Graham, E. B., Crump, A. R., Kennedy, D. W., Arntzen, E., Fansler, S., Purvine, S. O., Nicora, C. D.,
851   Nelson, W., Tfaily, M. M. and Stegen, J. C.: Multi 'omics comparison reveals metabolome
852   biochemistry, not microbiome composition or gene expression, corresponds to elevated biogeochemical
853   function in the hyporheic zone, Sci. Total Environ., 642, 742–753,
854   https://doi.org/10.1016/j.scitotenv.2018.05.256, 2018.

855

856   Grilli, J., Barabás, G., Michalska-Smith, M. J. and Allesina, S.: Higher-order interactions stabilize
857   dynamics in competitive network models, Nature, 548(7666), 210–213,
858   https://doi.org/10.1038/nature23273, 2017.

859

860   Hall, E. K., Bernhardt, E. S., Bier, R. L., Bradford, M. A., Boot, C. M., Cotner, J. B., del Giorgio, P. A.,
861   Evans, S. E., Graham, E. B., Jones, S. E., Lennon, J. T., Locey, K. J., Nemergut, D., Osborne, B. B.,
862   Rocca, J. D., Schimel, J. P., Waldrop, M. P. and Wallenstein, M. D.: Understanding how microbiomes
863   influence the systems they inhabit, Nat. Microbiol., 3(9), 977–982, https://doi.org/10.1038/s41564-018-

864 0201-z, 2018.
865
866 Homyak, P. M., Blankinship, J. C., Slessarev, E. W., Schaeffer, S. M., Manzoni, S. and Schimel, J. P.:
867 Effects of altered dry season length and plant inputs on soluble soil carbon, Ecology, 99(10), 2348–
868 2362, https://doi.org/10.1002/ecy.2473, 2018.
869
870 Jia, X., Dini-Andreote, F. and Falcão Salles, J.: Comparing the Influence of Assembly Processes
871 Governing Bacterial Community Succession Based on DNA and RNA Data, Microorganisms, 8(6), 798,
872 https://doi.org/10.3390/microorganisms8060798, 2020.
873
874 Jurburg, S. D., Nunes, I., Stegen, J. C., Le Roux, X., Priemé, A., Sørensen, S. J. and Salles, J. F.:
875 Autogenic succession and deterministic recovery following disturbance in soil bacterial communities,
876 Sci. Rep., 7(1), 1–11, https://doi.org/10.1038/srep45691, 2017.
877
878 Kaufman, M. H., Cardenas, M. B., Buttles, J., Kessler, A. J. and Cook, P. L. M.: Hyporheic hot
879 moments: Dissolved oxygen dynamics in the hyporheic zone in response to surface flow perturbations,
880 Water Resour. Res., 53(8), 6642–6662, https://doi.org/10.1002/2016WR020296, 2017.
881
882 Kearns, P. J., Angell, J. H., Howard, E. M., Deegan, L. A., Stanley, R. H. R. and Bowen, J. L.: Nutrient
883 enrichment induces dormancy and decreases diversity of active bacteria in salt marsh sediments, Nat.
884 Commun., 7(1), 12881, https://doi.org/10.1038/ncomms12881, 2016.
885
886 König, S., Worrich, A., Banitz, T., Centler, F., Harms, H., Kästner, M., Miltner, A., Wick, L. Y.,
887 Thullner, M. and Frank, K.: Spatiotemporal disturbance characteristics determine functional stability
888 and collapse risk of simulated microbial ecosystems, Sci. Rep., 8(1), 1–13,
889 https://doi.org/10.1038/s41598-018-27785-4, 2018.
890
891 Larned, S. T., Datry, T., Arscott, D. B. and Tockner, K.: Emerging concepts in temporary-river ecology,
892 Freshw. Biol., 55(4), 717–738, https://doi.org/10.1111/j.1365-2427.2009.02322.x, 2010.
893
894 LaRowe, D. E. and Van Cappellen, P.: Degradation of natural organic matter: A thermodynamic
895 analysis, Geochim. Cosmochim. Acta, 75(8), 2030–2042, https://doi.org/10.1016/j.gca.2011.01.020,
896 2011.
897
898 Leventhal, G. E., Ackermann, M. and Schiessl, K. T.: Why microbes secrete molecules to modify their
899 environment: the case of iron-chelating siderophores, J. R. Soc. Interface, 16(150), 20180674,
900 https://doi.org/10.1098/rsif.2018.0674, 2019.
901
902 Levy-Booth, D. J., Giesbrecht, I. J. W., Kellogg, C. T. E., Heger, T. J., D'Amore, D. V., Keeling, P. J.,
903 Hallam, S. J. and Mohn, W. W.: Seasonal and ecohydrological regulation of active microbial
904 populations involved in DOC, CO 2 , and CH 4 fluxes in temperate rainforest soil, ISME J., 13(4), 950–
905 963, https://doi.org/10.1038/s41396-018-0334-3, 2019.
906
907 Li, Y., Gao, Y., Zhang, W., Wang, C., Wang, P., Niu, L. and Wu, H.: Homogeneous selection dominates
908 the microbial community assembly in the sediment of the Three Gorges Reservoir, Sci. Total Environ.,
909 690, 50–60, https://doi.org/10.1016/j.scitotenv.2019.07.014, 2019.

910

911 Lloyd-Price, J., Arze, C., Ananthakrishnan, A. N., Schirmer, M., Avila-Pacheco, J., Poon, T. W.,
912 Andrews, E., Ajami, N. J., Bonham, K. S., Brislawn, C. J., Casero, D., Courtney, H., Gonzalez, A.,
913 Graeber, T. G., Hall, A. B., Lake, K., Landers, C. J., Mallick, H., Plichta, D. R., Prasad, M., Rahnavard,
914 G., Sauk, J., Shungin, D., Vázquez-Baeza, Y., White, R. A., Braun, J., Denson, L. A., Jansson, J. K.,
915 Knight, R., Kugathasan, S., McGovern, D. P. B., Petrosino, J. F., Stappenbeck, T. S., Winter, H. S.,
916 Clish, C. B., Franzosa, E. A., Vlamakis, H., Xavier, R. J. and Huttenhower, C.: Multi-omics of the gut
917 microbial ecosystem in inflammatory bowel diseases, Nature, 569(7758), 655–662,
918 https://doi.org/10.1038/s41586-019-1237-9, 2019.

919

920 Louca, S., Polz, M. F., Mazel, F., Albright, M. B. N., Huber, J. A., O'Connor, M. I., Ackermann, M.,
921 Hahn, A. S., Srivastava, D. S., Crowe, S. A., Doebeli, M. and Parfrey, L. W.: Function and functional
922 redundancy in microbial systems, Nat. Ecol. Evol., 2(6), 936–943, https://doi.org/10.1038/s41559-018-
923 0519-1, 2018.

924

925 Malik, A. A., Martiny, J. B. H., Brodie, E. L., Martiny, A. C., Treseder, K. K. and Allison, S. D.:
926 Defining trait-based microbial strategies with consequences for soil carbon cycling under climate
927 change, ISME J., 14(1), 1–9, https://doi.org/10.1038/s41396-019-0510-0, 2020.

928

929 Manzella, M., Geiss, R. and Hall, E. K.: Evaluating the stoichiometric trait distributions of cultured
930 bacterial populations and uncultured microbial communities, Environ. Microbiol., 21(10), 3613–3626,
931 https://doi.org/10.1111/1462-2920.14684, 2019.

932

933 Manzoni, S., Schimel, J. P. and Porporato, A.: Responses of soil microbial communities to water stress:
934 results from a meta-analysis, Ecology, 93(4), 930–938, https://doi.org/10.1890/11-0026.1, 2012.

935

936 Martínez, I., Stegen, J. C., Maldonado-Gómez, M. X., Eren, A. M., Siba, P. M., Greenhill, A. R. and
937 Walter, J.: The Gut Microbiota of Rural Papua New Guineans: Composition, Diversity Patterns, and
938 Ecological Processes, Cell Rep., 11(4), 527–538, https://doi.org/10.1016/j.celrep.2015.03.049, 2015.
939 Mauck, B. S. and Roberts, J. A.: Mineralogic Control on Abundance and Diversity of Surface-Adherent
940 Microbial Communities, Geomicrobiol. J., 24(3–4), 167–177,
941 https://doi.org/10.1080/01490450701457162, 2007.

942

943 McClain, M. E., Boyer, E. W., Dent, C. L., Gergel, S. E., Grimm, N. B., Groffman, P. M., Hart, S. C.,
944 Harvey, J. W., Johnston, C. A., Mayorga, E., McDowell, W. H. and Pinay, G.: Biogeochemical Hot
945 Spots and Hot Moments at the Interface of Terrestrial and Aquatic Ecosystems, Ecosystems, 6(4), 301–
946 312, https://doi.org/10.1007/s10021-003-0161-9, 2003.

947

948 Norland, S., Fagerbakke, K. M. and Heldal, M.: Light element analysis of individual bacteria by x-ray
949 microanalysis., Appl. Environ. Microbiol., 61(4), 1357–1362, https://doi.org/10.1128/AEM.61.4.1357-
950 1362.1995, 1995.

951

952 Ofiţeru, I. D., Lunn, M., Curtis, T. P., Wells, G. F., Criddle, C. S., Francis, C. A. and Sloan, W. T.:
953 Combined niche and neutral effects in a microbial wastewater treatment community, Proc. Natl. Acad.
954 Sci., 107(35), 15345–15350, https://doi.org/10.1073/pnas.1000604107, 2010.

955

956 Pérez Castro, S., Cleland, E. E., Wagner, R., Sawad, R. A. and Lipson, D. A.: Soil microbial responses
957 to drought and exotic plants shift carbon metabolism, ISME J., 13(7), 1776–1787,
958 https://doi.org/10.1038/s41396-019-0389-9, 2019.

960 Prosser, J. I. and Martiny, J. B. H.: Conceptual challenges in microbial community ecology, Philos.
961 Trans. R. Soc. B Biol. Sci., 375(1798), 20190241, https://doi.org/10.1098/rstb.2019.0241, 2020.
962 Ratzke, C., Denk, J. and Gore, J.: Ecological suicide in microbes, Nat. Ecol. Evol., 2(5), 867–872,
963 https://doi.org/10.1038/s41559-018-0535-1, 2018.

965 Romaní, A. M., Vázquez, E. and Butturini, A.: Microbial Availability and Size Fractionation of
966 Dissolved Organic Carbon After Drought in an Intermittent Stream: Biogeochemical Link Across the
967 Stream–Riparian Interface, Microb. Ecol., 52(3), 501–512, https://doi.org/10.1007/s00248-006-9112-2,
968 2006.

970 Sengupta, A., Stegen, J. C., Neto, A. A. M., Wang, Y., Neilson, J. W., Tatarin, T., Hunt, E., Dontsova,
971 K., Chorover, J., Troch, P. A. and Maier, R. M.: Assessing Microbial Community Patterns During
972 Incipient Soil Formation From Basalt, J. Geophys. Res. Biogeosciences, 124(4), 941–958,
973 https://doi.org/10.1029/2017JG004315, 2019a.

975 Sengupta, A., Indivero, J., Gunn, C., Tfaily, M. M., Chu, R. K., Toyoda, J., Bailey, V. L., Ward, N. D.
976 and Stegen, J. C.: Spatial gradients in the characteristics of soil-carbon fractions are associated with
977 abiotic features but not microbial communities, Biogeosciences, 16(19), 3911–3928,
978 https://doi.org/10.5194/bg-16-3911-2019, 2019b.

980 Shu, D., Guo, J., Zhang, B., He, Y. and Wei, G.: rDNA- and rRNA-derived communities present
981 divergent assemblage patterns and functional traits throughout full-scale landfill leachate treatment
982 process trains, Sci. Total Environ., 646, 1069–1079, https://doi.org/10.1016/j.scitotenv.2018.07.388,
983 2019.

985 Slater, L. D., Ntarlagiannis, D., Day-Lewis, F. D., Mwakanyamale, K., Versteeg, R. J., Ward, A.,
986 Strickland, C., Johnson, C. D. and Lane, J. W.: Use of electrical imaging and distributed temperature
987 sensing methods to characterize surface water–groundwater exchange regulating uranium transport at
988 the Hanford 300 Area, Washington, Water Resour. Res., 46(10),
989 https://doi.org/10.1029/2010WR009110, 2010.

991 Song, H.-S., Stegen, J. C., Graham, E. B., Lee, J.-Y., Garayburu-Caruso, V. A., Nelson, W. C., Chen,
992 X., Moulton, J. D. and Scheibe, T. D.: Representing Organic Matter Thermodynamics in
993 Biogeochemical Reactions via Substrate-Explicit Modeling, bioRxiv, 2020.02.27.968669,
994 https://doi.org/10.1101/2020.02.27.968669, 2020.

996 Starnawski, P., Bataillon, T., Ettema, T. J. G., Jochum, L. M., Schreiber, L., Chen, X., Lever, M. A.,
997 Polz, M. F., Jørgensen, B. B., Schramm, A. and Kjeldsen, K. U.: Microbial community assembly and
998 evolution in subseafloor sediment, Proc. Natl. Acad. Sci., 114(11), 2940–2945,
999 https://doi.org/10.1073/pnas.1614190114, 2017.

1001 Stegen, J. C., Lin, X., Konopka, A. E. and Fredrickson, J. K.: Stochastic and deterministic assembly

1002 processes in subsurface microbial communities, ISME J., 6(9), 1653–1664,
1003 https://doi.org/10.1038/ismej.2012.22, 2012.
1004
1005 Stegen, J. C., Lin, X., Fredrickson, J. K., Chen, X., Kennedy, D. W., Murray, C. J., Rockhold, M. L. and
1006 Konopka, A.: Quantifying community assembly processes and identifying features that impose them,
1007 ISME J., 7(11), 2069–2079, https://doi.org/10.1038/ismej.2013.93, 2013.
1008
1009 Stegen, J. C., Lin, X., Fredrickson, J. K. and Konopka, A. E.: Estimating and mapping ecological
1010 processes influencing microbial community assembly, Front. Microbiol., 6,
1011 https://doi.org/10.3389/fmicb.2015.00370, 2015.
1012
1013 Stegen, J. C., Konopka, A., McKinley, J. P., Murray, C., Lin, X., Miller, M. D., Kennedy, D. W., Miller,
1014 E. A., Resch, C. T. and Fredrickson, J. K.: Coupling among Microbial Communities, Biogeochemistry
1015 and Mineralogy across Biogeochemical Facies, Sci. Rep., 6(1), 1–14, https://doi.org/10.1038/srep30553,
1016 2016.
1017
1018 Stegen, J. C., Bottos, E. M. and Jansson, J. K.: A unified conceptual framework for prediction and
1019 control of microbiomes., Curr. Opin. Microbiol., https://doi.org/10.1016/j.mib.2018.06.002, 2018a.
1020
1021 Stegen, J. C., Johnson, T., Fredrickson, J. K., Wilkins, M. J., Konopka, A. E., Nelson, W. C., Arntzen,
1022 E. V., Chrisler, W. B., Chu, R. K., Fansler, S. J., Graham, E. B., Kennedy, D. W., Resch, C. T., Tfaily,
1023 M. and Zachara, J.: Influences of organic carbon speciation on hyporheic corridor biogeochemistry and
1024 microbial ecology, Nat. Commun., 9(1), 1–11, https://doi.org/10.1038/s41467-018-02922-9, 2018b.
1025
1026 Thompson, L. R., Sanders, J. G., McDonald, D., Amir, A., Ladau, J., Locey, K. J., Prill, R. J., Tripathi,
1027 A., Gibbons, S. M., Ackermann, G., Navas-Molina, J. A., Janssen, S., Kopylova, E., Vázquez-Baeza, Y.,
1028 González, A., Morton, J. T., Mirarab, S., Zech Xu, Z., Jiang, L., Haroon, M. F., Kanbar, J., Zhu, Q., Jin
1029 Song, S., Kosciolek, T., Bokulich, N. A., Lefler, J., Brislawn, C. J., Humphrey, G., Owens, S. M.,
1030 Hampton-Marcell, J., Berg-Lyons, D., McKenzie, V., Fierer, N., Fuhrman, J. A., Clauset, A., Stevens,
1031 R. L., Shade, A., Pollard, K. S., Goodwin, K. D., Jansson, J. K., Gilbert, J. A. and Knight, R.: A
1032 communal catalogue reveals Earth's multiscale microbial diversity, Nature, 551(7681), 457–463,
1033 https://doi.org/10.1038/nature24621, 2017.
1034
1035 Tripathi, B. M., Stegen, J. C., Kim, M., Dong, K., Adams, J. M. and Lee, Y. K.: Soil pH mediates the
1036 balance between stochastic and deterministic assembly of bacteria, ISME J., 12(4), 1072–1083,
1037 https://doi.org/10.1038/s41396-018-0082-4, 2018.
1038
1039 Wagner, M.: Single-cell ecophysiology of microbes as revealed by Raman microspectroscopy or
1040 secondary ion mass spectrometry imaging, Annu. Rev. Microbiol., 63, 411–429,
1041 https://doi.org/10.1146/annurev.micro.091208.073233, 2009.
1042
1043 Wallenstein, M. D. and Hall, E. K.: A trait-based framework for predicting when and where microbial
1044 adaptation to climate change will affect ecosystem functioning, Biogeochemistry, 109(1), 35–47,
1045 https://doi.org/10.1007/s10533-011-9641-8, 2012.
1046
1047 Wang, J., Shen, J., Wu, Y., Tu, C., Soininen, J., Stegen, J. C., He, J., Liu, X., Zhang, L. and Zhang, E.:

Phylogenetic beta diversity in bacterial assemblages across ecosystems: deterministic versus stochastic processes, ISME J., 7(7), 1310–1321, https://doi.org/10.1038/ismej.2013.30, 2013.

Whitman, T., Neurath, R., Perera, A., Chu-Jacoby, I., Ning, D., Zhou, J., Nico, P., Pett-Ridge, J. and Firestone, M.: Microbial community assembly differs across minerals in a rhizosphere microcosm, Environ. Microbiol., 20(12), 4444–4460, https://doi.org/10.1111/1462-2920.14366, 2018.

Wieder, W. R., Allison, S. D., Davidson, E. A., Georgiou, K., Hararuk, O., He, Y., Hopkins, F., Luo, Y., Smith, M. J., Sulman, B., Todd-Brown, K., Wang, Y.-P., Xia, J. and Xu, X.: Explicitly representing soil microbial processes in Earth system models, Glob. Biogeochem. Cycles, 29(10), 1782–1800, https://doi.org/10.1002/2015GB005188, 2015.

Wisnoski, N. I., Muscarella, M. E., Larsen, M. L., Peralta, A. L. and Lennon, J. T.: Metabolic insight into bacterial community assembly across ecosystem boundaries, Ecology, 101(4), e02968, https://doi.org/10.1002/ecy.2968, 2020.

Wu, W., Lu, H.-P., Sastri, A., Yeh, Y.-C., Gong, G.-C., Chou, W.-C. and Hsieh, C.-H.: Contrasting the relative importance of species sorting and dispersal limitation in shaping marine bacterial versus protist communities, ISME J., 12(2), 485–494, https://doi.org/10.1038/ismej.2017.183, 2018.

Zachara, J. M., Long, P. E., Bargar, J., Davis, J. A., Fox, P., Fredrickson, J. K., Freshley, M. D., Konopka, A. E., Liu, C., McKinley, J. P., Rockhold, M. L., Williams, K. H. and Yabusaki, S. B.: Persistence of uranium groundwater plumes: Contrasting mechanisms at two DOE sites in the groundwater–river interaction zone, J. Contam. Hydrol., 147, 45–72, https://doi.org/10.1016/j.jconhyd.2013.02.001, 2013.

Zhou, J. and Ning, D.: Stochastic Community Assembly: Does It Matter in Microbial Ecology?, Microbiol. Mol. Biol. Rev., 81(4), https://doi.org/10.1128/MMBR.00002-17, 2017.

Zhou, J., Liu, W., Deng, Y., Jiang, Y.-H., Xue, K., He, Z., Nostrand, J. D. V., Wu, L., Yang, Y. and Wang, A.: Stochastic Assembly Leads to Alternative Communities with Distinct Functions in a Bioreactor Microbial Community, mBio, 4(2), https://doi.org/10.1128/mBio.00584-12, 2013.
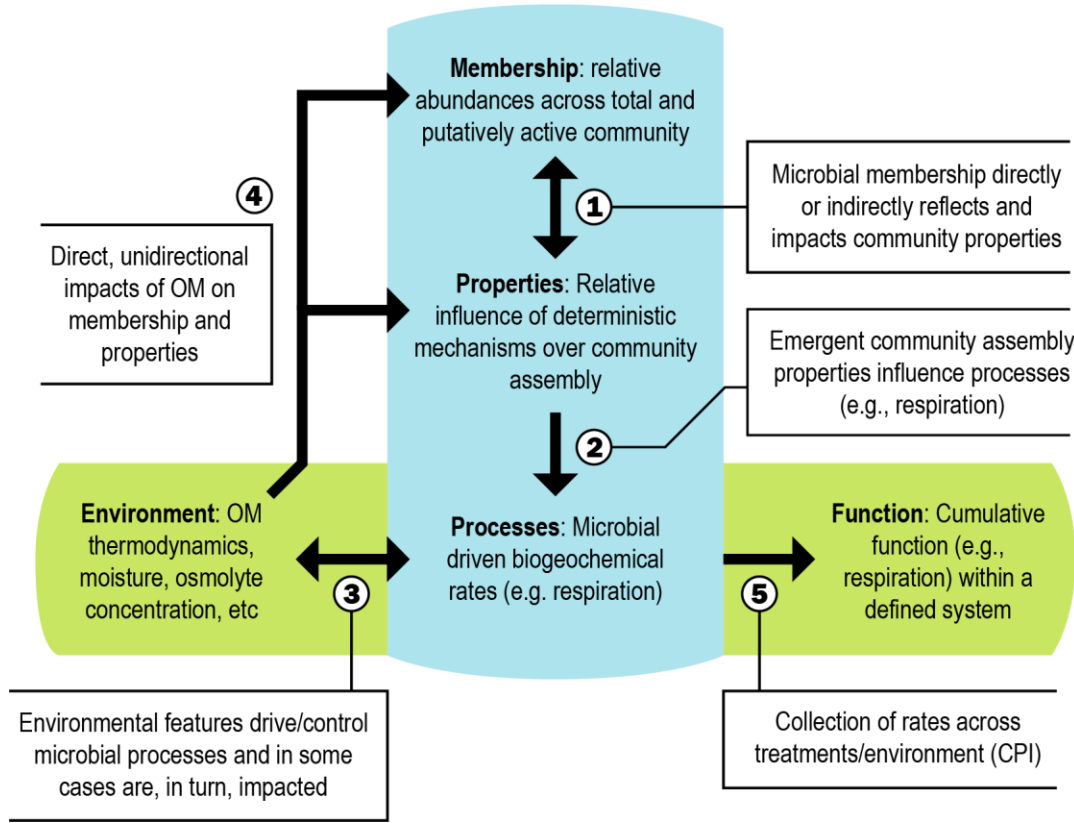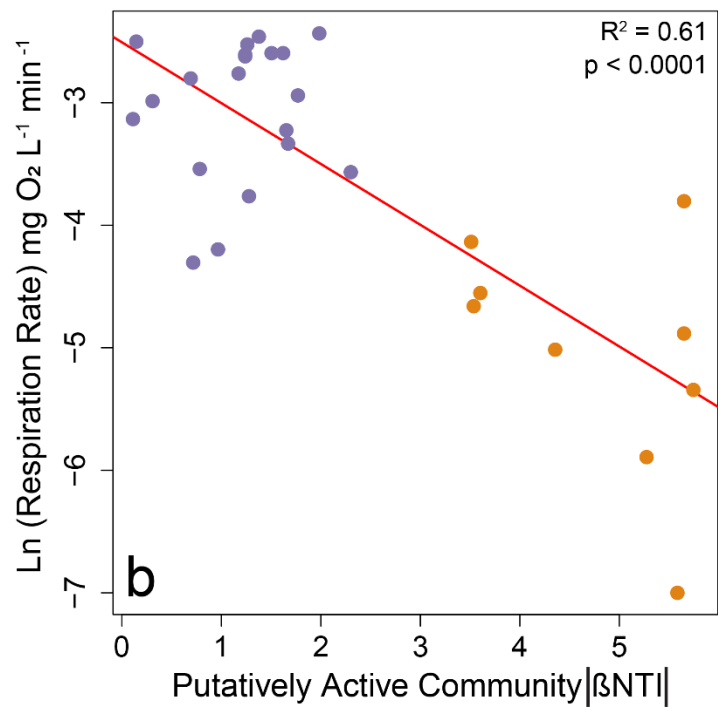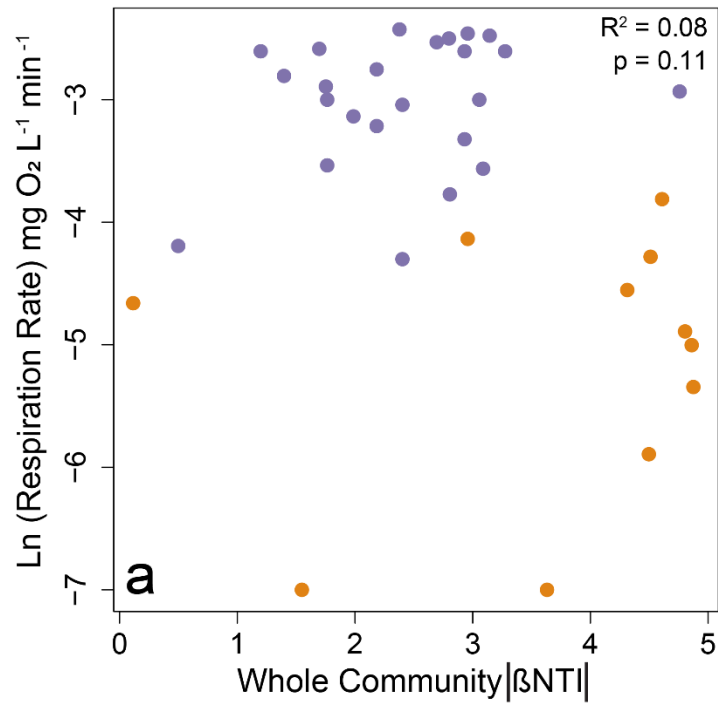
1084
1085
1086 **Figure 1. Integrated conceptual framework.** The conceptual figure (modified from Hall et al. (2018))
1087 details relationships (indicated by numbered arrows) between cumulative properties of the microbial
1088 community (*e.g.*, microbial membership, community assembly properties, biogeochemical rates),
1089 environmental features [*e.g.*, organic matter (OM) thermodynamics], and emergent ecosystem function
1090 [e.g., control point influence (CPI)]. Double headed arrows indicate feedbacks.
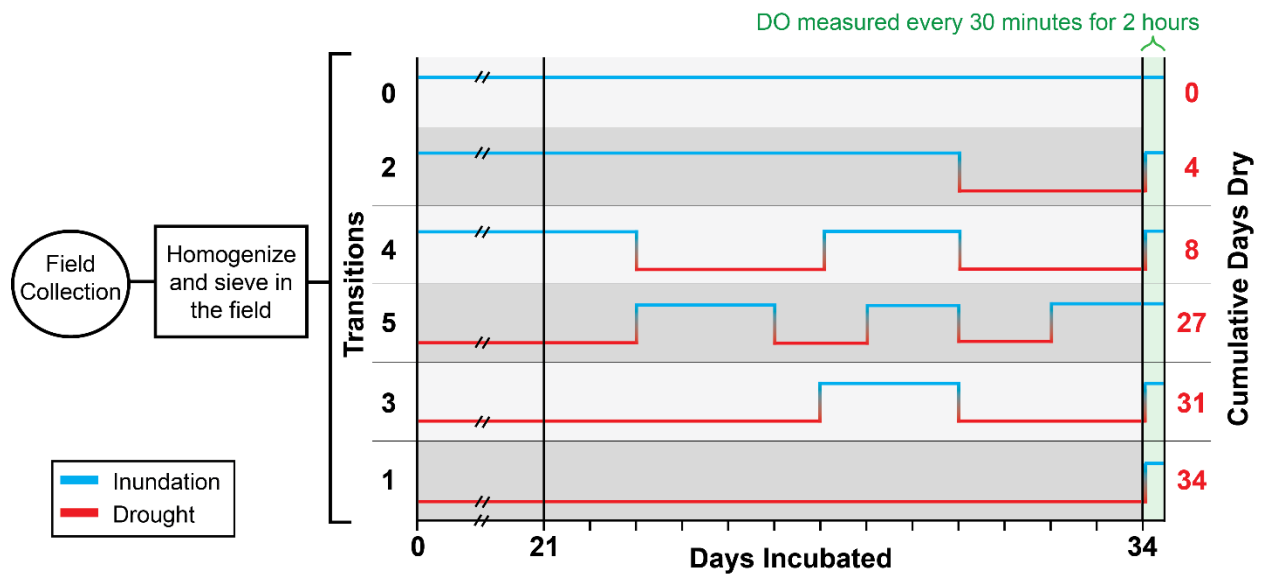
1091
1092
1093
1094 **Figure 2. Experimental design of batch reactor incubations subjected to six treatment regimes**
1095 **of inundated (blue line) and dry (red line) conditions.** Black values on the left indicate the number of
1096 inundated/dry transitions, including the final inundation that all treatments experienced immediately
1097 prior to the measurement of respiration. Red values on the right indicate the number of cumulative dry
1098 days (e.g., treatments with 1 or 3 transitions experienced 34 or 31 cumulative dry days, respectively.
1099 Transitions between inundated and dry conditions started on day 24. All treatments were held at either
1100 an inundated or dry state prior to day 24. Treatments are ordered by the number of days dry.
1101

Figure 3. Natural log transformed respiration rates (i.e., O₂ consumption) as a function of the absolute value of βNTI for (a) whole communities or (b) putatively active communities. Larger absolute values of βNTI indicate stronger influences of deterministic assembly. Nonlinearity was observed because the respiration rate has a lower limit of 0 such that its relationship with βNTI was fit as a negative exponential function. The significant regression model is shown as a red line, and statistics are provided on each panel. Treatments with 0, 4, 8, or 27 days dry are shown in purple. Treatments with 31or 34 days dry are shown in orange.

41
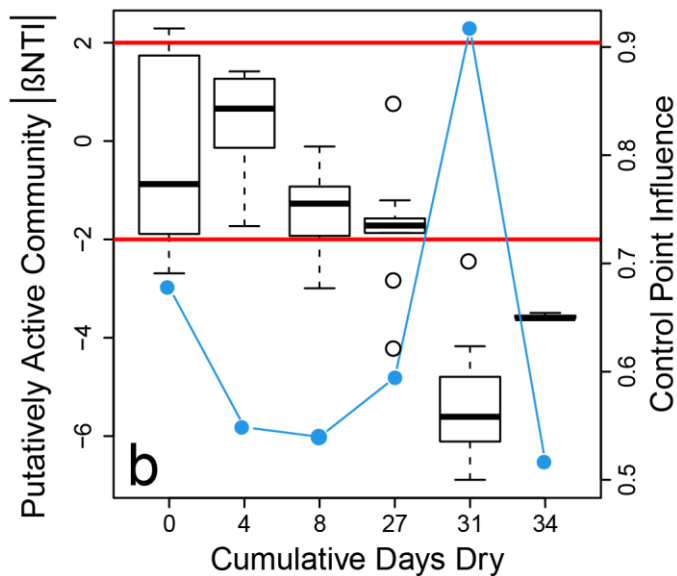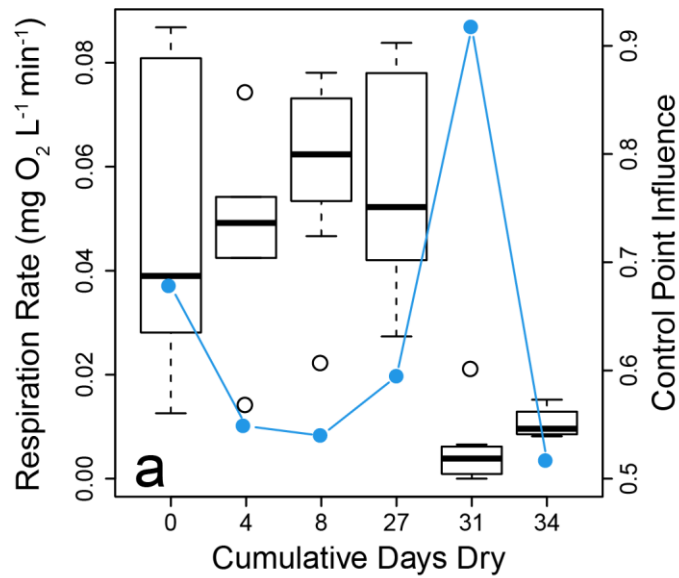
Figure 4. Boxplot representations of respiration rate (a) and putatively active community βNTI (b) distributions as a function of the cumulative number of days reactors were in a dried state. Each value along the horizontal axis represents a different experimental treatment. On both panels the right hand axis provides estimates of control point influence (blue circles and lines) across the treatments. Horizontal red lines in (b) indicate significance thresholds; values below -2 indicate deterministic homogenous selection, values above +2 indicate deterministic variable selection, and values between -2 and +2 indicate stochastic assembly.
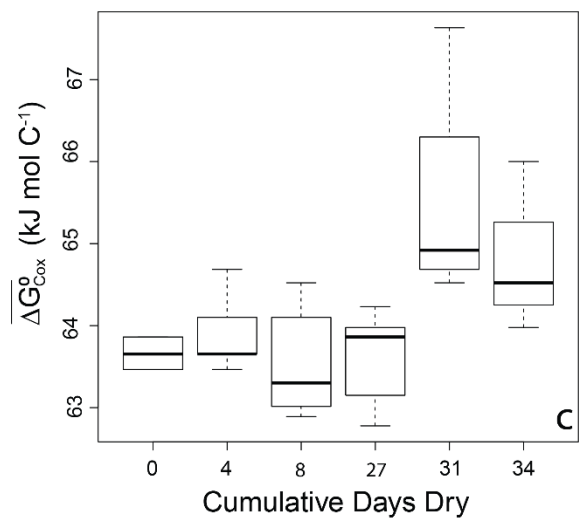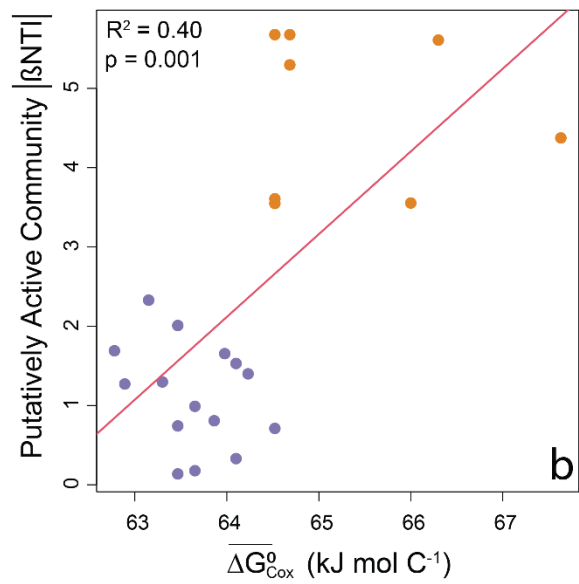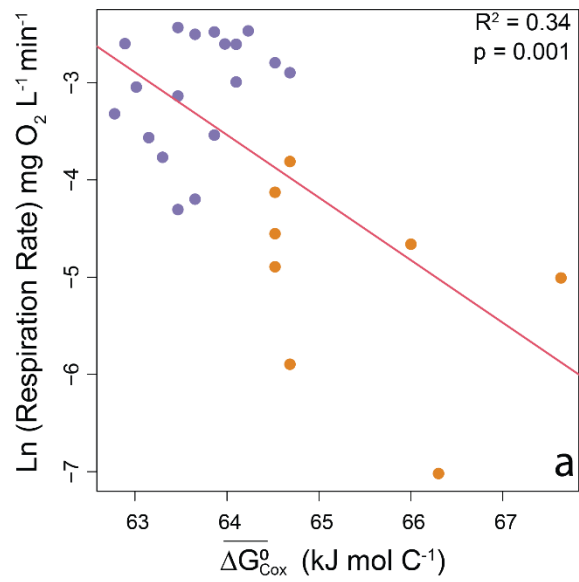
Figure 5. Microbial processes and properties as a function of OM thermodynamics, and impacts of disturbance on OM thermodynamics. (a) Respiration rates (natural log transformed) decreased with decreasing favorability for oxidation (larger values of ΔG^0_{Cox}). (b) The strength of deterministic selection measured as the absolute value of βNTI increased with decreasing favorability for oxidation. Regression models are shown as red lines and statistics are provided on each panel. (c) Boxplot representations of the distributions of OM thermodynamics across experimental treatments. Significant increases were observed for treatments with 31 or 34 cumulative dry days. See text and Figure S7 for a description of statistics. Treatments with 0, 4, 8, or 27 days dry are shown in purple. Treatments with 31or 34 days dry are shown in orange.
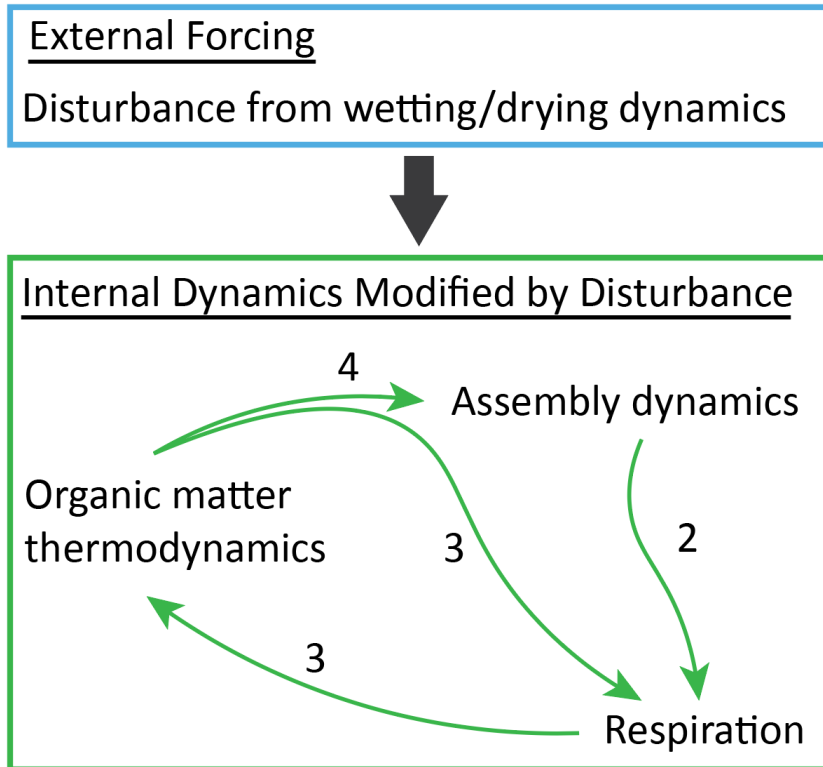
Figure 6. Integrated conceptual interpretation of results from this study. Collectively, our results indicate that the external forcing imposed by disturbance leads to feedback between assembly of the putatively active community and respiration rates that is modulated by coupled dynamics in organic matter thermodynamics. Relative to Fig. 1, here external and internal aspects of the environment are separated. The arrows within the internal dynamics component are analogous to arrows 2,3, and 4 in Figure 1. The arrow from external to internal is not considered in Figure 1, and represents the impact of external forcing on all aspects of the internal system. These impacts are both direct effects of disturbance and indirect effects mediated through the internal feedback that collectively lead to impacts of re-wetting that are contingent on desiccation history.